Account/Revue

Crystal chemistry of aluminium carboxylates: From molecular species towards porous infinite three-dimensional networks

Thierry Loiseau [a],[*],[1], Christophe Volkringer [a],[b], Mohamed Haouas [c], Francis Taulelle [c], Gérard Férey [c]

[a] Unité de catalyse et chimie du solide, UMR CNRS 8181, Université de Lille, bâtiment C7, BP 90108, 59652 Villeneuve-d'Ascq, France
[b] Institut universitaire de France (IUF), 1, rue Descartes, 75231 Paris, France
[c] Institut Lavoisier, UMR CNRS 8180, Université de Versailles–Saint-Quentin, 45, avenue des États-Unis, 78035 Versailles, France

ABSTRACT

This account describes the crystal chemistry of aluminium in association with O-donor organic ligands, such as polycarboxylates. In this overview, molecular assemblies of aluminium-based species are discussed from the background knowledge of the polycationic species occurring in aqueous solution. The use of hydro/solvothermal synthetic route has led to the generation of novel crystalline extended three-dimensional networks, of metal-organic frameworks (MOFs) type, with consequent porosity properties. The first illustration of such materials was the aluminium-containing MIL-53 (Materials Institute Lavoisier – number 53), obtained from the hydrothermal reaction of aluminium salt source with terephthalic acid. This finding gave rise to the development of new series of porous aluminium MOF-like materials, some of which are now produced at the industrial scale. This review presents a description of various crystalline structures, from a classification based on the nuclearity of the aluminium-centered building units, involved in the construction of the framework.

© 2015 Académie des sciences. Published by Elsevier Masson SAS. All rights reserved.

1. Introduction

Since 1989 [1], the study of the association of metallic centers with chelating polydentate O- or N-donor organic linkers has led to a new and very topical class of solids, now known as metal-organic frameworks (MOF) or coordination polymers (or coordination network solids [2]). These solids, often three-dimensional and porous, are thermally stable and robust, and serve as host functionalized matrices for diverse applications, such as gas storage, molecular separation, drug delivery, catalytic reactors,

batteries, thin films shaping... [3–6]. They conjugate the physical and chemical properties of both the inorganic and organic parts for providing multifunctional materials, and use in particular the pore geometry of the three-dimensional framework.

Almost all the metallic atoms of the periodic table can incorporate the framework. Historically, most of the early works reported the use of divalent transition metals (i.e. Zn^{2+}, Cu^{2+}...). It was further extended to tri-, tetra- and even pentavalent cations with the same success. Among them, trivalent metals were very promising, particularly the crystallized solids of the MIL-100/MIL-101 series [7–9], based on aluminium, chromium and iron which exhibited the first large mesoporous cavities in a framework. Among them, aluminium deserved a special attention due to its lightweight and its cheap cost, when thinking to industrial production for gas storage applications, for instance. For

us, it was an opportunity to better understand the chemistry of aluminium from the knowledge of the species [7,8,10] which can exist, and which can be used to design novel three-dimensional topologies.

Aluminium is first one of the most abundant metallic elements on earth's crust (8.3% by weight) and is generally encountered in natural minerals, such as feldspars, zeolites, micas. The bauxite-type rocks are the most commonly source in the aluminium extraction process for producing the Al metal.

In aqueous solution, aluminium predominantly exists with the oxidation state of +3, complexed by anionic charged species, although the low valence state (+1) has also been explored with the discovery of a specific chemistry [11]. Depending on the pH values, the Al coordination ranges from six (octahedral at low pH) to four (tetrahedral at high pH). The intermediate five-fold coordination (trigonal bipyramid), less usual, is now well described in natural minerals (andalusite [12,13], grandedierite [14], yoderite [15], etc.), organic complexes [16,17] or organically templated open-framework aluminophosphates [18,19]. The recently observed [20] aqueous molecular form $(Al(OH)(H_2O)_4{}^{2+})$, specific to aluminium chemistry, is in contrast with other trivalent metals.

Due to their amphoteric behavior [21], aluminium hydroxides are generally dissolved in acidic solutions (pH < 3; $Al(H_2O)_6{}^{3+}$) or near-neutral and basic solutions (pH > 8; $Al(OH)_4{}^-$). Its trivalent charge associated to the small ionic radius (0.53 Å in tetrahedra, or 0.675 Å for octahedra [22]) leads to hard cations with a strong Lewis acid character. It implies a strong reactivity with Lewis bases, like OH^-, F^-, $PO_4{}^{3-}$, $SO_4{}^{2-}$, but also with organic O- or N-donor ligands (R-O^-, R-COO^- or R-NH_2…), with the formation of various species resulting from hydrolysis and/ or complexation processes. Some recent works have reported calculations about the analyses of electronic structure of aluminium (or more generally group 13 elements) compared to those of trivalent transition metals [23]. In the case of the six-coordinate systems, they showed that the p elements exhibit electron-rich hypervalent bonding, without any role for the d orbitals, which the major difference with transition metals. Consequently, the Al-based compounds would be thermodynamically more stable and kinetically more reactive than those bearing neighbouring trivalent transition metals.

Most of the works related to the aluminium chemistry concern three main application domains: formation of polycations, biochemistry of aluminium and preparation of alumina ceramics.

Polycationic moieties [24] are soluble molecular oligomeric compounds coming from the hydrolysis of the aquohydroxo species $[Al(OH)_h(H_2O)_{N-h}]^{(3-h)+}$ in water. An accurate control of their condensation gives rise to the formation of isolated nanoclusters with different nuclearities. In case of $h = 3$, the condensation leads to the precipitation of the hydroxide or oxyhydroxide phases. These researches were concentrated on the narrow range of existence of these polynuclear complexes because of specific properties of flocculation in water treatment processes. In particular, they act as efficient coagulants for the removal of some pollutants and turbidity. They can

also be intercalated into layered clay-like solids, such as Montmorillonite with the production after heating treatment of pillared compounds used efficiently in heterogeneous catalysis. They are also found in antiperspirants, as adjuvants for vaccine formulation or dye mordants (see review article by Casey [24]).

The reactivity of aluminium in biological systems is also a significant field of research since Al is assumed to exhibit a neurotoxic activity [25–28]. This fact is due, for instance, to the observation of the abnormally high concentration of aluminium in brain tissues coming from patients developing an Alzheimer's disease or other degenerative neurologic processes, but its direct role into the mechanism of the formation of these specific diseases is still debating. Nevertheless, the role of aluminium in cellular systems is well documented and this leads to the exploration of biochemical models for which a large number of molecular complexes have been investigated.

In the last domain, different types of alumina are usually industrially produced from precipitation and calcination processes of forms of aluminium hydroxides. They find many applications as ceramics, composite materials or catalysts.

The knowledge of these different aspects of the aluminium chemistry was the starting point for attempting to build up extended infinite network with aluminium centers for potential areas of applications. This review will first present the state-of-the-art on the different molecular Al-based clusters which can be used as building blocks for the discovery of new MOF-type networks using various carboxylates linkers. They are described in the second part.

2. Aluminium polycationic species

Several reviews [24,29] have well described this aspect. One may just briefly summary this topic by listing the different aqueous species which have been isolated so far.

The cationic 'blocks' consist of several Al atoms connected to each other through oxo and hydroxo groups. The coordination of aluminium-center (usually 6) is often completed by aquo ligands in terminal positions. These species, very soluble in water, crystallize in the presence of counter anions (sulfates, selenates, etc.) for a certain degree of hydrolysis. Several types of oligomeric clusters have been discovered, mainly in the sixties, by Johansson [27].

The first cationic moiety is (Fig. 1a) the dinuclear unit $[Al_2(OH)_2(H_2O)_8]^{4+}$ (called Al_2J) [30]. It crystallizes with sulfates or selenates from slow evaporation of aqueous solutions. It contains two octahedrally coordinated aluminium atoms sharing a μ_2-OH edge. A second oligomer, more recently found (it took seven years for getting a crystal!), was obtained during the preparation of the dimeric species Al_2J with sulfates [31]. The octamer is composed of eight six-fold coordinated aluminium centers $[Al_8(OH)_{14}(H_2O)_{16}]^{10+}$ (Fig. 1b). Connections are ensured via two μ_3-OH and four μ_2-OH ligands. This central four-membered unit is corner-shared through μ_2-OH with four additional peripheral AlO_6 polyhedra.

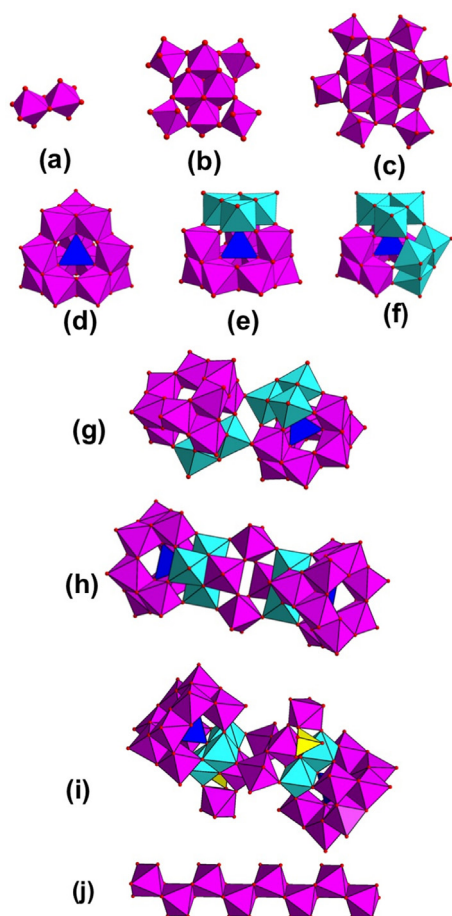The best known polycationic oligomer belongs to the Baker–Figgis–Keggin isomer family. In it, a central MO_4

Fig. 1. (Color online.) Aluminum polycationic species crystallizing from an aqueous solution. (a) Al_2J: $[Al_2(OH)_2(H_2O)_8]^{4+}$; (b) Al_8: $[Al_8(OH)_{14}(H_2O)_{16}]^{10+}$; (c) M-Al_{13}: $[Al_{13}(OH)_{24}(H_2O)_{24}]^{15+}$; (d) ε-Al_{13}: $[AlO_4Al_{12}(OH)_{24}(H_2O)_{12}]^{7+}$; (e) δ-Al_{13}: $[AlO_4Al_{12}(OH)_{24}(H_2O)_{12}]^{7+}$; (f) γ-Al_{13}: $[AlO_4Al_{12}(OH)_{25}(H_2O)_{11}]^{6+}$; (g) Al_{26}: $[Al_{26}O_8(OH)_{50}(H_2O)_{20}]^{12+}$; (h) Al_{30}: $[Al_{30}O_8(OH)_{56}(H_2O)_{24}]^{18+}$; (i) Al_{32}: $[Al_{32}O_8(OH)_{60}(H_2O)_{28}(SO_4)_2]^{16+}$; (j) Al_2-∞: $[Al_2(OH)_4(H_2O)_4]^{2+}$.

tetrahedron is capped with four trimers of edge-sharing MO_6 octahedra. Five isomers exist. They depend on the 60° rotation of one trimer M_3O_{13} to each other, giving rise to corner-sharing connection in the α configuration [29] (adopted with high valence cations (W^{6+}, Mo^{6+}) in the tetrahedron) and edge-sharing linkage in the ε configuration. An intermediate connection (x via edges/x–4 via corner) occurs in three other isomers (β, γ, δ).

Discovered by Johansson [32–35], the Al_{13} unit (or $[AlO_4Al_{12}(OH)_{24}(H_2O)_{12}]^{7+}$) adopts the ε isomer (Fig. 1d). The ε-Al_{13} exists in two forms (cubic or monoclinic), depending on the number (four or three) of counter anions sulfates or selenates. Within the Al_{13} cluster, the central AlO_4 tetrahedron is connected via corner-sharing μ_4-O to the trimers Al_3O_{13}, the latter being connected to each other via corner-sharing μ_2-OH. Note that in the δ isomer, isolated by Rowsell and Nazar [36] and Abeysinghe et al. [37], the structure around the central AlO_4 is similar except the orientation of one of the four trimers which is rotated by 60° (Fig. 1e). The γ isomer (Fig. 1f), resulting from an

additional 60° rotation of a second trimer, has also been isolated recently [38]. Note that another isomer exists, but only in highly concentrated chloride medium (Cl/Al = 15/13 in the structure). Different from the Keggin configuration (Fig. 1c), the flat M-Al_{13} cluster [39] ($[Al_{13}(OH)_{24}(H_2O)_{24}]^{15+}$) is built up from one central AlO_6 octahedron, surrounded by six peripheral AlO_6 octahedra through μ_3-OH edge-sharing connection. These peripheral AlO_6 octahedra are linked to each other via μ_2-OH edge-sharing bridges. This seven-membered core is then connected to six other AlO_6 octahedra forming an outer shell via μ_2-OH corner-sharing.

The α-Al_{13} building block can also be embedded in a larger cation containing for example silicates anions as in the natural mineral Zunyite ($Al_{13}Si_5O_{20}(OH)_{16}F_2Cl$) [40]. Another large aluminium polycation, simultaneously reported by two teams [36,41], corresponds to the so-called Al_{30} molecule ($[Al_{30}O_8(OH)_{56}(H_2O)_{24}]^{18+}$). Obtained by heating a solution of ε-Al_{13} at 85 °C, it also exists in a millimolar solution of ε-Al_{13} [29]. It gathers two δ-Al_{13} motifs, connected to each other through a ring of four corner-sharing AlO_6 octahedra (Fig. 1h). More recently, $[Al_{32}O_8(OH)_{60}(H_2O)_{28}(SO_4)_2]^{16+}$ (or Al_{32}) [42] has been isolated from a solution of a $AlCl_3$/NaOH mixture at 70 °C, then heated at 150 °C under mild hydrothermal conditions. Addition of Na_2SO_4 to the resulting solution at room temperature gave rise to the crystallization of Al_{32} after one week. Its structure is close to that of Al_{30} (Fig. 1i). In Al_{32}, two additional AlO_6 octahedra link via corner-sharing mode, the Al_{13} subunit and the central ring of four AlO_6 ring. One of the terminal oxo groups is also sharing with a sulfate anion. This chemical system has been investigated in the presence of 2,6-naphthalenedisulfonate, used as counter-anionic moiety for the crystallization of such polycationic species during the hydrolysis process [37]. This crystallization route has successfully led to the isolation of the δ-Al_{13} and Al_{30} motifs. Moreover, a novel polycation, Al_{26} ($[Al_{26}O_8(OH)_{50}(H_2O)_{20}]^{12+}$; Fig. 1g) has been obtained. It consists of the association of two δ-Al_{13} structural units via four μ_2-hyroxyl groups from the trimeric Al_3 subunits, which have been rotated (60°) in order to generate the δ form.

Finally, a distinct assembly of aluminium cations is also built up from infinite polymeric network based on chains $[Al_2(OH)_4(H_2O)_4]^{2+}$ [43] (Fig. 1j) intercalated by halides anions (I, Br, Cl) (obtained from heating process at 75 °C followed by microfiltration). In this system, the AlO_6 octahedral units are connected to each other through edge-sharing with a *cis* mode in order to generate a zigzag ribbon structure. This chain-like motif may play the role of a precursor for the formation of aluminium hydroxide $Al(OH)_3$ (gibbsite or nordstrandite). More generally, many studies report the possible links between these molecular polycationic species in aqueous solution and their role in the generation of solid phases of aluminium oxy(hydro-xi)des involving infinite condensation process [44,45].

3. Aluminium carboxylates in molecular assemblies

The biological role of aluminium incited many researchers to investigate its interactions with 'model' organic

molecules in order to understand its potential role on the development of dialysis, dementia or neurodegenerative pathologies, such as Alzheimer disease. A large number of studies have then focused on its speciation with small organic ligands in solution, for identifying the role of aluminium. Many molecular species stabilized with molecules containing carboxylate function were then isolated and characterized by means of X-ray diffraction and NMR (^{27}Al) techniques. The reviews by Salifoglou [46] or Mensinger et al. [47] propose their classification as a function of their nuclearity. These aluminium-based species were used as building units in the following for the construction of extended infinite networks in (Al)MOF-type solids.

3.1. Mononuclear motifs

They are numerous. They can be classified as a function of the number of carboxylate functions bonded to aluminium, usually found in octahedral coordination.

The first organic ligand of this series is stabilized by the hydroxy mono acid CH$_3$CH(OH)COOH (lactic acid = H$_2$lact) [48]. Three lactate ligands are linked to Al via their hydroxyl group. The connection of the fourth lactate is ensured by one of the deprotonated carboxyl oxygen atoms (monodentate mode). The same mode occurs with glycolate (HOCH$_2$COO$^-$) [49,50] or quinolate ((HO)$_4$C$_6$H$_2$COO$^-$) [51]. In the glycolate-based cluster, strong hydrogen interactions occur between the hydroxy groups of two aluminium-centered octahedra, generating well defined pairs of monomeric units.

The other complexes involves two carboxylates groups, including the oxalate (C$_2$O$_4$$^{2-}$ = ox) and malonate moieties (CH$_2$(COO$^-$)$_2$ = mal), the first members of the aliphatic α,ω-dicarboxylates. The aluminium oxalate [Al(ox)$_3$]$^{3-}$ (Fig. 2a),

obtained in the presence of different counter-cations [52–56], is stabilized by three chelating organic ligands. With the malonate [Al(mal)$_2$(η-H$_2$O)$_2$]$^-$ [57], only two molecules are connected to aluminium through the two carboxyl oxygen of the carboxylate group (bidentate mode). The octahedral coordination is completed by the addition of two terminal water molecules. A similar situation is encountered in two molecular compounds with the derived complexing agent, methylmalonate [58,59] (CH$_3$CH(COO$^-$)$_2$). In one of them, terminal water molecules are replaced by methanol groups [59].

Other complexes have been obtained with bis(imino)-diacetate (= ida) [60,61], bis(methylimino)diacetate [62] or tricarboxylates (nitrilotriacetate = nta [63]) with binary or tertiary imino groups. Aluminium cation is bonded to both carboxyl oxygen and imino nitrogen atoms. This leads to a tridendate or tetradentate connection of the organic molecules.

Citrate anion, present in human blood, is a tricarboxylate with a central hydroxyl group (($^-$OOC)CH$_2$C(OH)(COO$^-$)CH$_2$COO$^-$ = cit) with many possible binding sites, and extremely reactive toward Al. Among the various possibilities of connection, one of them, the monomer ([Al(cit)$_2$]$^{5-}$), crystallizes at pH 8 with two citrate molecules in a tridentate fashion [64,65]. Aluminium is surrounded by four carboxyl oxygen atoms and two central hydroxyl groups. The third carboxylate function remains free, but still deprotonated. A similar complex ([Al(cit)(Hcit)]$^{4-}$) is still stable at lower pH (4–6), but the free carboxylates of one of two citrates become protonated [65]. Finally, edta [66,67] (ethylenediamine tetraacetate), also provides a mononuclear unit. It is bonded to aluminium through its four carboxylates and two amino groups, and ensures the octahedral coordination of aluminium.
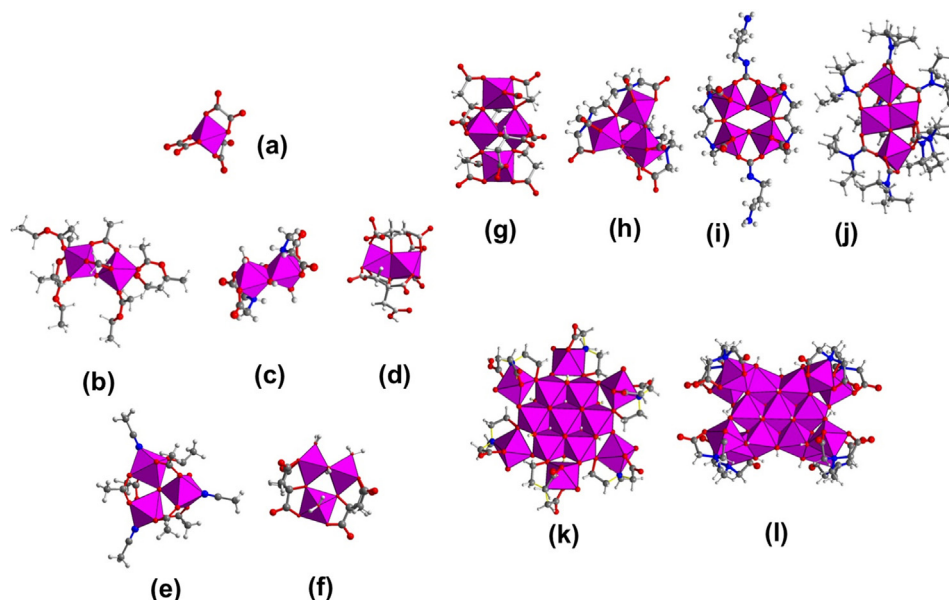

Fig. 2. (Color online.) Polyhedral representations of the molecular species of aluminium carboxylates with various nuclearities. (a) Al(oxalate)$_3$; (b) [Al$_2$(μ_2-OH)(CH$_3$CO$_2$)$_2$(CH$_3$COOC$_2$H$_5$)$_6$]$^{3+}$; (c) [Al$_2$(μ_2-OH)$_2$(ida)$_2$(η-H$_2$O)$_2$]^0; (d) [Al$_2$(cit)(Hcit)$_2$]$^{4-}$; (e) [Al$_3$(μ_3-O)(O$_2$C-CCH$_3$)$_6$(CH$_3$CN)$_3$]$^+$; (f) [Al$_3$(μ_2-OH)$_2$(cit)$_2$(η-H$_2$O)$_4$]$^-$; (g) [Al$_4$(μ_2-OH)$_2$(L-C$_4$H$_3$O$_5$)$_4$(η-H$_2$O)$_4$]$^{2-}$; (h) [Al$_4$(μ_2-OH)$_4$(hpdta)$_2$]$^{2-}$; (i) [Al$_4$(μ_2-O)(μ_2-OH)(hpdta)$_2$(O$_2$CNHC$_3$H$_6$NH$_3$)$_2$]$^-$; (j) [Al$_4$(μ_3-O)$_2$(O$_2$CNC(CH$_3$)$_2$)$_8$] (k) [Al$_{13}$(μ_3-OH)$_6$(OH)$_{12}$(heidi)$_6$]$^{3+}$; (l) [Al$_{15}$(μ_3-O)$_4$(μ_3-OH)$_6$(OH)$_{14}$(hpdta)$_4$]$^{3-}$.

We may also note the occurrence of an isolated hexa-aquo aluminium species ($[Al(\eta\text{-}H_2O)_6]^{3+}$) crystallizing in the presence of mellitate groups (natural mineral Mellite) [68]. The cohesion of the crystal structure is only ensured by the hydrogen bond interactions between the bonded water and carboxylate functions of the benzene hexacarboxylate.

3.2. Dinuclear motifs

Three types of bridging mode occur in the aluminium dinuclear Al_2 moieties. In most of the cases, the octahedrally coordinated aluminium centers have a common edge. The only exception to this rule, corresponding to a corner-sharing of Al octahedra, is provided by the mixed ethylacetate acetate [69] $[Al_2(\mu_2\text{-}OH)(CH_3CO_2)_2(CH_3\text{-}COOC_2H_5)_6]^{3+}$ (Fig. 2b). Both acetate groups play the role of bridging groups between the metallic centers in this cluster.

Otherwise, edge-sharing is observed, with two μ_2-hydroxo groups as in the nitrilotriacetate [63] $[Al_2(\mu_2\text{-}OH)_2(nta)_2]^{3-}$ or bis(imino)diacetate [60,70] $[Al_2(\mu_2\text{-}OH)_2(ida)_2(\eta\text{-}H_2O)_2]^0$ or ethylenediaminetetraacetate [71] (edta) $[Al_2(\mu_2\text{-}OH)_2(edta)(\eta\text{-}H_2O)_2]^0$ complexes (Fig. 2c). Monomeric species have also been observed with these complexing agents [60,61,63]. In other examples, the μ_2-hydroxo groups of the edge-sharing are replaced by μ_2-oxo ones coming from the alcoholate oxygen atoms of the N-(2-hydroxyethyl)iminodiacetate (= heidi) [72] $[Al_2(heidi)_2(\eta\text{-}H_2O)_2]^0$ or the saccharate [73] ligands $[Al_2(C_6H_6O_8)_2(\eta\text{-}H_2O)_2]^{2-}$. The octahedral surrounding is ensured with the bonding of one terminal water molecule except with the nta species, for which a nitrogen atom participates to the coordination sphere of aluminium. Similar situations are found in the ida and heidi complexes, in which a nitrogen atom (located in trans position to water with ida and cis position with heidi) is bonded to aluminium.

Face-sharing bridging mode also exists (Fig. 2d) with the citrate complex [74] $[Al_2(cit)(Hcit)_2]^{4-}$, stabilized at rather low pH (≈ 3.5), in contrast to the monomer obtained at higher pH (4–8) [64,65]. The alcoholate oxygen atoms of the three distinct citrates with different protonation states are bridging the aluminium cations to each other.

3.3. Trinuclear motifs

The building units based on three aluminium centers exhibit two very different types of connectivity. The first is cationic. Discovered for the first time in 1944 [75], it is rather common for di- and trivalent 3d transition metals, such as trivalent Cr^{3+}, Mn^{3+}, Co^{3+}, Ru^{3+}, Rh^{3+}, Ir^{3+}, Pt^{3+} [76] or divalent ones (Mn^{2+}, Fe^{2+}, Co^{2+}, Ni^{2+}) [77]. Surprisingly, the first trimer containing a block IIIA element was isolated in 1992 with gallium [78], and later on, the indium analog was identified in 2006 [79]. The aluminium analog was only discovered in 2002 by Roesky et al. [80] $[Al_3(\mu_3\text{-}O)(O_2C\text{-}CF_3)_6(THF)_3]^+$ and 2006 by Bekaert et al. [81] $[Al_3(\mu_3\text{-}O)(O_2C\text{-}CCH_3)_6(CH_3CN)_3]^+$ using non-aqueous solvents. Other similar compounds were also reported more recently [82]. This cationic complex

consists of three AlO_6 units connected to each other through a central μ_3-oxo group, in a triangular plane (Fig. 2e). The acetates (or trifluoroacetate) bridge the aluminium cations via their oxygen located in the equatorial plane of the octahedron. The O- (THF) or N-donor (CH_3CN) groups of the organic solvent molecules occupy the apical site, in trans position with the μ_3-oxo ligand.

The anionic form exists with the citrate ligand, either at relatively high pH (≈ 9) [83] with a 1:1 Al/cit ratio ($[Al_3(\mu_2\text{-}OH)(cit)_3(\eta\text{-}H_2O)]^{4-}$) or, unexpectedly, at very low pH (1.2–3.0), with [84] a 3:2 Al/cit ratio ($[Al_3(\mu_2\text{-}OH)_2(cit)_2(\eta\text{-}H_2O)_4]^-$). In both Al_3 cores (Fig. 2f), two octahedrally coordinated aluminium polyhedra share an edge (μ_2-hydroxo groups at low pH or μ_2-oxo groups coming from the deprotonated alcoholate groups at high pH). The third AlO_6 octahedron shares one corner [μ_2-oxo groups coming from the deprotonated alcoholate groups of two distinct citrates (low pH) or one μ_2-oxo together with one μ_2-hydroxo group (high pH) with the common edge of the dimer. The edge-sharing species are μ_2-hydroxo groups (low pH) or μ_2-oxo groups coming from the deprotonated alcoholate groups (high pH)]. Thus, according to the conditions of synthesis, three different nuclearities (monomeric, dimeric or trimeric) are offered with for citrate-Al complexes, which can be used for building new (Al)MOFs.

3.4. Tetranuclear motifs

Four types of tetrameric building units are evidenced for the aluminium carboxylates. Two of them exhibit exclusively corner-sharing, the two others involving both corner- and edge-sharing.

Concerning corner-sharing, two situations are observed using both the ligand derived from the hydroxypropyldiaminotetracetic acid (H_5hpdta). It corresponds to two diaminoacetic functions linked by a hydroxypropyl group, and can be viewed as a heidi derivative.

A first complex $[Al_4(\mu_2\text{-}OH)_4(hpdta)_2]^{2-}$ is tetrahedral. It is described [60] from the corner-sharing connection of four AlO_6 octahedra, linked to each other through μ_2-hydroxo or μ_2-oxo groups (Fig. 2h). Within this $Al_4(OH)_4O_2$ core, the aluminium centers are located at each corners of the tetrahedral motif since the μ_2-OH groups occupy the middle of four of the six edges of the tetrahedral motif. The two remaining edges are μ_2-oxo groups from the deprotonated hydroxyl function of two distinct ligands. The octahedral coordination of aluminium is either completed by carboxyl oxygen or nitrogen atoms.

The second Al_4 core [60,85] $[Al_4(\mu_2\text{-}O)(\mu_2\text{-}OH)(hpdta)_2(O_2CNHC_3H_6NH_3)_2]^-$ is defined by a tetragonal plane with four AlO_6 octahedra. They are linked to each other via corner-sharing μ_2-oxo and μ_2-hydroxo groups, or μ_2-oxo from the deprotonated hydroxyl function of the hpdta ligand (Fig. 2i). Beside the bonding of aluminium with the carboxylate and nitrogen of hpdta, two additional carbamate molecules (generated from the reaction of CO_2 and proylenediamine, present in the starting solution) also bridge two adjacent metallic centers via their carboxylate functions.

Two other complexes $[Al_4(\mu_2\text{-}OH)_2(\text{L-}C_4H_3O_5)_4(\eta\text{-}H_2O)_4]^{2-}$ (i) and $[Al_4(\text{DL-}C_4H_3O_5)_6]^{6-}$ (ii) have been isolated at different pH values (3.5 and 6, respectively) with the malate molecule [86] and are built up from an identical tetranuclear arrangement (Fig. 2g). It consists of two central AlO_6 octahedra joined by a common edge, which can be a $\mu_2\text{-}OH$ in (i) or $\mu_2\text{-}O$ in (ii). This dimeric unit is further connected to two additional AlO_6 octahedra through corner-sharing μ_2-oxo from the deprotonated hydroxyl malate ligand. In a way, it can be regarded as an extended version of the trinuclear unit obtained with citrate [83,84], with the connection of a fourth AlO_6 octahedra. In one of two complexes, only the L-form of the chiral malate is bonded to aluminium, with four terminal water molecules located to the two additional corner-sharing AlO_6 units. In the second one, a racemic mixture of the L- and D-forms occurs around the Al_4O_6 core.

The fourth configuration is reported in the aluminium *N,N*-diisopropylacetate [87] $[Al_4(\mu_3\text{-}O)_2(O_2CNC(CH_3)_2)_8]$ and consists of two AlO_5 trigonal bipyramids linked via a common oxo edge (Fig. 2j). Two AlO_6 octahedra are also linked through corners to the resulting μ_3-oxo species. The acetate ligands bridge two adjacent aluminium metals in a bidentate mode, but two of them are in chelating mode with the two external aluminium atoms. This inorganic motif is related to that found in other aluminium-based compounds complexed with phosphates (AlPO$_4$-15 [88–90]). In the latter, it corresponds to the building unit encountered in the natural mineral leucophosphite [91] (iron phosphate), for which the metallic cations are all octahedrally coordinated.

3.5. Polynuclear motifs

The use of carboxylate also favors the condensation of the metallic cations with the formation of molecular moieties showing high nuclearity. The two largest aluminium carboxylates are related to the flat conformation of the Al_{13} polycation [39]. The topology of the first complex is identical to the polycationic species Al_{13} and stabilized by six ligands involving iminodiacetate function such as the *heidi* linker ($[Al_{13}(\mu_3\text{-}OH)_6(OH)_{12}(heidi)_6]^{3+}$) [72]. In this tridecanuclear compound (Fig. 2k), the tetradentate *heidi* binder replaces the terminal water molecules as well as one of the μ_2–OH corners of the six peripheral aluminium-based octahedra found in the flat polycation Al_{13} (each *heidi* ligand is associated to one external AlO_6 unit). The substitution of the terminal aquo species from the polycation Al_{13} [39] occurs either through the carboxyl oxygen or nitrogen atoms of the *heidi* molecule.

The second polynuclear species $[Al_{15}(\mu_3\text{-}O)_4(\mu_3\text{-}OH)_6(OH)_{14}(hpdta)_4]^{3-}$ is obtained with the *ligand hpdta* [92] (Fig. 2l) and consists of a derived version of the previous one, with the occurrence of four pairs of AlO_6 octahedral units in the peripheral ring, linked via both corner- and edge-sharing to the inner seven-membered core (identical to that of the flat Al_{13} motif). Each set of bi-octahedral units is complexed by one *hpdta* ligand, which acts as heptadentate molecule. This induces the bonding of carboxyl oxygen and nitrogen atoms with the eight peripheral aluminium cations in the pentadecanuclear brick. The Al_{15} negatively-charged moieties are stabilized with piperazinium cations, which promote a supramolecular assembly with a three-dimensional arrangement reminiscent to that found in the zeolite frameworks. From these structural considerations, it was observed that large channels with 11 Å diameter are crossing with cavities with 5 Å diameter.

Following the observations with the polycations series, large molecular systems have been also reported with gallium and carboxylate linkers. In particular, the use of acetate in methanol or 1,3-propanediol gives rise to the formation of "wheel-shape" building blocks containing ten or eighteen gallium centers [93], respectively. This type of molecular ring-type configuration is known with a large number of metallic elements. In the "gallic wheels", the gallium centers have six-fold octahedral surrounding and connected to each other via a common edge. In the Ga_{18} ring, some of the gallium atoms are also found in five-fold coordination. For the other gallium carboxylates, similar complexes to those encountered with aluminium have been prepared by using different carboxylates (oxalate, citrate, *heidi*…) [55,65,78,85,94,95].

4. Aluminum-based metal-organic frameworks (MOFs)

The richness of the reactivity of divalent or trivalent metals with polycarboxylate ligands [6] incited us to use for the first time aluminium for generating MOF-like porous networks. The first report in 2004 of such a hybrid solid [96]: MIL-53(Al), (MIL standing for Materials of Institute Lavoisier number 53) described the reaction under hydrothermal mild conditions (220 °C for 72 h) of an aluminium nitrate source ($Al(NO_3)_3 \cdot 9H_2O$) in an aqueous solution of terephthalic acid. Its open structure is built up from infinite chains of AlO_6 octahedral units, connected to each other through the terephthalate linkers, in order to generate 1D lozenge-shape channels. This pioneering work opened the way to the isolation of a new family of MOF-type compounds bearing *p* block elements, in particular with aluminium. Férey's group had previously reported similar structure types with transition metals, such as vanadium or chromium [97,98].

This strategy was then successfully extended to other aluminium-based MOFs, using synthesis protocols operating under mild hydro(or solvo)-thermal conditions ($T > 100$ °C). This fruitful method, previously used for the templated synthesis of microporous aluminophosphates (AlPO$_4$-*n*) [99], provides solids which differ from the polynuclear molecular assemblies described above, which are usually obtained at room temperature after slow evaporation process. It slightly differs also from the method leading to aluminium carboxylates, precursors of further ceramics. They are obtained at 100 °C or boiling values of the organic solvents used for the synthesis at normal pressure.

The following paragraphs describe a classification of the different types of topologies, dependent on the nature and nuclearity of the aluminium-based building units, obtained by this method.

4.1. Metal-organic frameworks with mononuclear or dinuclear building units

Discrete motifs of aluminium centers are rarely encountered in the MOF-type compounds. Indeed, only one illustration of isolated AlO_6 octahedral units has been described in a three-dimensional framework synthesized in the presence of 1,3,5-benzenetrisbenzoic acid (H_3btb). The structure of this compound, $Al(btb)$ or CAU-4 (CAU stands for Christian-Albrechts-Universität) [100], is isotypic with scandium-based MOFs [101,102]. It is based on the single AlO_6 units connected through the carboxylate arms of the tritopic ligand, in a bidentate fashion with a twisted face-to-face manner. It results in the generation of infinite hybrid chains with the $\cdots$Al–O–C–O–Al–O–C–O–Al$\cdots$ sequence, which are then connected to each other via the trisbenzoate backbone. The ternary symmetry of the tritopic organic molecule induces the formation of a honeycomb network with one-dimensional channels of diameter ~ 9.6 Å, and a BET surface area of $1520 \, m^2/g$.

A second example of isolated inorganic motifs has been reported in a dinuclear molecular complex $Al_2(OH)_2(H_2O)_2(2,4,6-Hptc)_2$ crystallizing with 2,4,6-pyridine tricarboxylic acid (2,4,6-H_3ptc) [103]. It consists of the two aluminium centers connected via edge-sharing mode (μ_2-OH). The octahedral coordination environment of aluminium is composed of two OH groups, one aquo species in terminal position, two carboxyl oxygen atoms and one nitrogen atom from the pyridine-based ligand. The third carboxylate arm of the organic molecule remained under its protonated form in this complex, but a second compound, CAU-16 ($Al(OH)\{Al(2,4,6-ptc)(OH)(H_2O)\}_2$), was identified with the unprotonated organic tricarboxylate [103]. It still consists of the same dinuclear subunit ($Al_2(OH)_2(H_2O)_2$), but the remaining unprotonated carboxylate arm is connected to a second type of inorganic subunit, containing infinite chains of $AlO_4(OH)_2$ octahedral units (trans connection type via the μ_2-OH groups). It results in the formation of three-dimensional network with channels of 10–11 Å. Surprisingly, no nitrogen adsorption was observed in CAU-16, but the capacity of CO_2 storage has been measured, with a maximum of 1.76 mmol/g at 196 K.

4.2. Metal-organic frameworks with trinuclear building units

This type of unit (three $AlO_5(OH,H_2O)$ octahedral units sharing a corner through a central μ_3-oxo group) was previously reported as isolated molecular species, stabilized by monodentate carboxylate ligands [80,81] (Fig. 2e).

Such a trimeric building block was encountered for the first time in MIL-96(Al) [104] or $Al_{12}O(OH)_{12}\{(OH)_4(H_2O)_5\}(1,3,5-btc)_6 \cdot nH_2O$, using trimesic acid (1,3,5-H_3btc). Its structure is built up from the association of the trinuclear μ_3-oxo centered clusters 'Al$_3$O' with chains of $AlO_2(OH)_4$ and $AlO_4(OH)_2$ octahedra, leading to a honeycomb layered sub-network forming 18-membered rings. The cohesion of the three-dimensional framework is ensured by the trimesate ligands, which link the two types of distinct inorganic bricks. This unusual connection mode generates the existence of three types of cavities (free

diameter of 8–9 Å maximum; volumes of 750, 450 and 100 Å^3), encapsulating free water molecules or isolated aluminium cations. BET surface area in MIL-96(Al) was $487 \, m^2/g$.

This phase is hydrothermally obtained for a relatively wide range of pH (1–3), but a second solid (($Al_3O(OH)(H_2O)_2(1,3,5-btc)_2 \cdot nH_2O$)) crystallizes in the same system. Observed only for pH values in the range 0.5–0.7, its structure [105] is isostructural with the MIL-100 series (Fe, Cr, V...) [6] and only contains the trinuclear μ_3-oxo centered clusters 'Al$_3$O' as building units. The MIL-100(Al) framework is based on these 'Al$_3$O' clusters linked to each other via the tritopic molecules 1,3,5-btc (Fig. 3) and represents an augmented version of the zeolite ZSM-39 [106] (or MTN code [107]) based on SiO_4 tetrahedra. Indeed, the assembly of these 'Al$_3$O' units replaces the O atoms of the SiO_4, with linking trimesates located on each face of the super-tetrahedron. The latter share their vertices and lead to a three-dimensional system of channels with sizes of 5.2 and 8.8 Å, which shows two distinct types of cavities. The small cages ($\oslash$: 25 Å) are delimited by 12 pentagonal rings defining a dodecahedral geometry (5^{12}); the large cages ($\oslash$: 29 Å) are delimited by 12 pentagonal rings and 4 hexagonal rings corresponding to a hexakaidodecahedral geometry ($5^{12}6^4$). Incidentally, note that, whereas the structure of the MIL-100(Cr) [7] was elucidated by means of modeling tools combined with high XRD powder data, the atomic arrangement in MIL-100(Al) was determined by single-crystal XRD analysis from an original microdiffraction setup (ESRF synchrotron radiation beamline ID13, Grenoble, France), allowing the collection of intensity data from a tiny crystal of $2 \times 2 \times 2 \, \mu m$ size [105]. Upon heating, NMR and IR analyses [108,109] show that only one of the terminal water species attached to the aluminium center are evacuated, generating a coordinatively unsaturated site, with a five-fold environment for aluminium.

The MTN zeotype MIL-101(Al) ($Al_3O(NH_2\_1,4-bdc)_3(DMF)_3(Cl) \cdot xDMF$) was also isolated with a functionalized ditopic linker: the 2-amino terephthalic acid ($NH_2\_1,4-H_2bdc$) [110,111]. This topology, firstly obtained with pure terephthalic acid reacting with Cr^{3+} [8], exits with aluminium only when an unfunctionalized linker is used in DMF medium. Closely related to that found in MIL-100, it consists of trinuclear μ_3-oxo centered 'Al$_3$O' subunits linked through the 2-amino terephthalate molecule, forming super-tetrahedral bricks (Fig. 3) in which, this time, the ditopic molecule is located at the edge of the so-called super-tetrahedron. The dimensions of the windows allowing access to the center of the cages are larger (12 Å for the small cage ($\oslash$: 29 Å this time) and 16 Å for the larger one ($\oslash$: 34$\oslash$Å)). The specific BET surface area is about $2100 \, m^2/g$ for both $NH_2\_MIL-101(Al)$ and MIL-100(Al) [105,111].

A second phase ($Al_3O(NH_2\_1,4-bdc)_3(DMF)_3(AlCl_4) \cdot xDMF$) appeared during the attempts to isolate the MIL-101(Al) analog [110]. Its structure, related to the MIL-88 type [112,113] (also called later MOF-235 [114]), is built up from the 'Al$_3$O' subunits connected to the ditopic linker and generates a new periodic framework with hexagonal pores channels together with bipyramidal cages, with trimeric
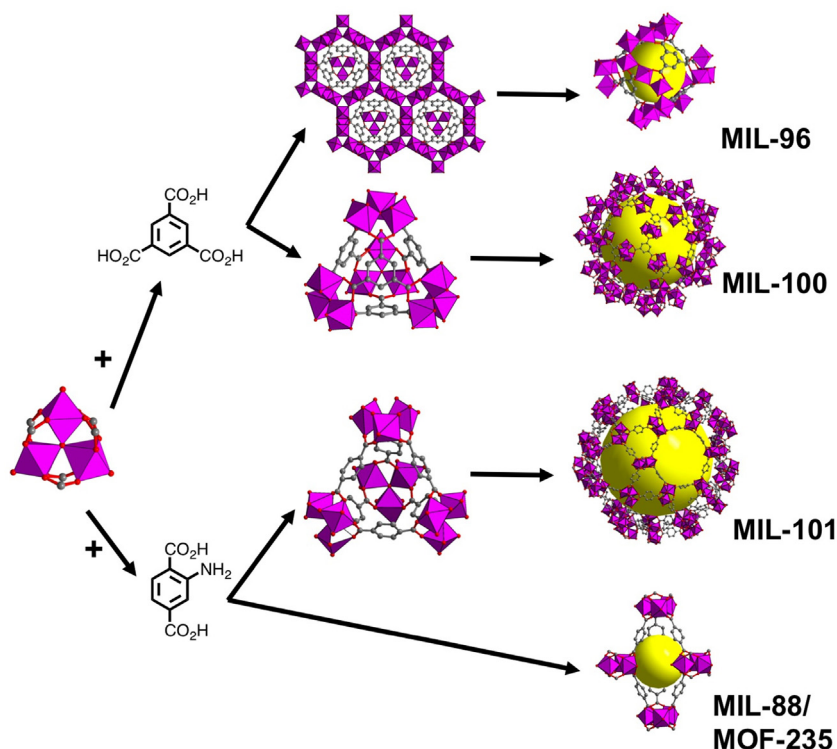
Fig. 3. (Color online.) View of the trinuclear μ_3-oxo centered building unit 'Al$_3$O' (left). Views of the network of MIL-96(Al), super-tetrahedral units, obtained from the association with trimesate (MIL-100) or 2-amino-terephthalate (MIL-101) linker (middle). Representation of cavities in MIL-96, MIL-100, MIL-101 and MIL-88/MOF-235 (right). NH$_2$ group has been omitted for clarity. Yellow spheres indicate the pore space.

units at each vertex (Fig. 3). Many ditopic ligands with different lengths adopt this structure type. The cavity of the MIL-88 topology is able to host a wide range of solvents, which induce a large swelling effect (up to 300% cell volume), depending on the nature of the trapped species [113]. The NH$_2$_MIL-101(Al) and NH$_2$_MIL-88(Al) appeared to be two kinetically controlled phases [110,115] before the formation of the NH$_2$_MIL-53(Al) [116,117]. Depending on the DMF/water (DMF = N,N-dimethylformamide) content, the NH$_2$_MIL-101(Al) phase crystallizes in pure DMF solvent, whereas the NH$_2$_MIL-88(Al) phase appears in the mixed DMF/water solvent. In this chemical system with AlCl$_3$·6H$_2$O as a precursor, it seems that the NH$_2$_MIL-88(Al) is formed first and then transformed into NH$_2$_MIL-101(Al) due to the presence of a H–Cl·DMF complex, which promotes its formation [118]. Such a structural transition of MIL-53/MIL-88 sequence was also previously described in the iron(III) terephthalate system [119].

4.3. Metal-organic frameworks with octanuclear building units

In the system with trimesic acid, a third phase crystallized with MIL-100(Al) and MIL-96(Al). This compound: (MIL-110(Al) [120,121]) exists either for very acidic pH values (∼ 0) for short reaction times (< 5 h) or at higher pH values (3.5–4.0) for longer times (> 50 h). MIL-110(Al) (formula Al$_8$(OH)$_{12}${(OH)$_3$(H$_2$O)$_3$}(1,3,5-btc)$_3$·nH$_2$O) is obtained under the form of tiny hexagonal elongated crystals (1–15 μm), which have also been analyzed structurally by

using the already mentioned single-crystal microdiffraction setup from ESRF (synchrotron radiation beamline ID13, Grenoble, France). The structure is built up from discrete octanuclear motifs composed of three dinuclear subunits of AlO$_2$(OH)$_3$(H$_2$O) or AlO$_2$(OH)$_4$ edge-shared octahedra, linked by corners to two AlO$_3$(OH)$_3$ octahedra (Fig. 4). This new inorganic cationic entity [Al$_8$(OH)$_{12}${(OH)$_3$(H$_2$O)$_3$}]$^{9+}$ is then linked to the trimesate ligands, which give rise to a 3D honeycomb-like lattice with large channels of diameter 16 Å (BET surface value: 1400 m^2/g), satisfying the symmetry of both the trimesate and the octahedral units. The benzene rings of the trimesate linker are located along the wall of the channels.

A second compound: Al$_4$(OH)$_2$(OMe)$_4$(NH$_2$_1,4-bdc)$_3$·xH$_2$O (or CAU-1 [122]), obtained in methanol medium, exhibits a structure also based on an octanuclear unit, but different from the previous one. Its structure (Fig. 4) is described from the assembly of octameric bricks, consisting of 8-membered ring of AlO$_3$(OMe)$_2$(OH) octahedral units, which are connected through corner-sharing (μ_2-OH) or edge-sharing connection (μ_2-OMe) mode, in alternation. This wheel-like motif is new for aluminium, but was previously encountered with trivalent transition metals (V^{3+}, Cr^{3+} and Fe^{3+}) in molecular assemblies [123–125]. Each 8-ring is linked to each other through 12 ditopic ligands in order to create a three-dimensional network (bcc-type packing) based on the compact stacking of octahedral ($\varnothing \approx 10$ Å) and tetrahedral ($\varnothing \approx 4.5$ Å) cavities. The corresponding BET surface area is 1370 m^2/g. The methoxy group (from methanol used as solvent) bridges
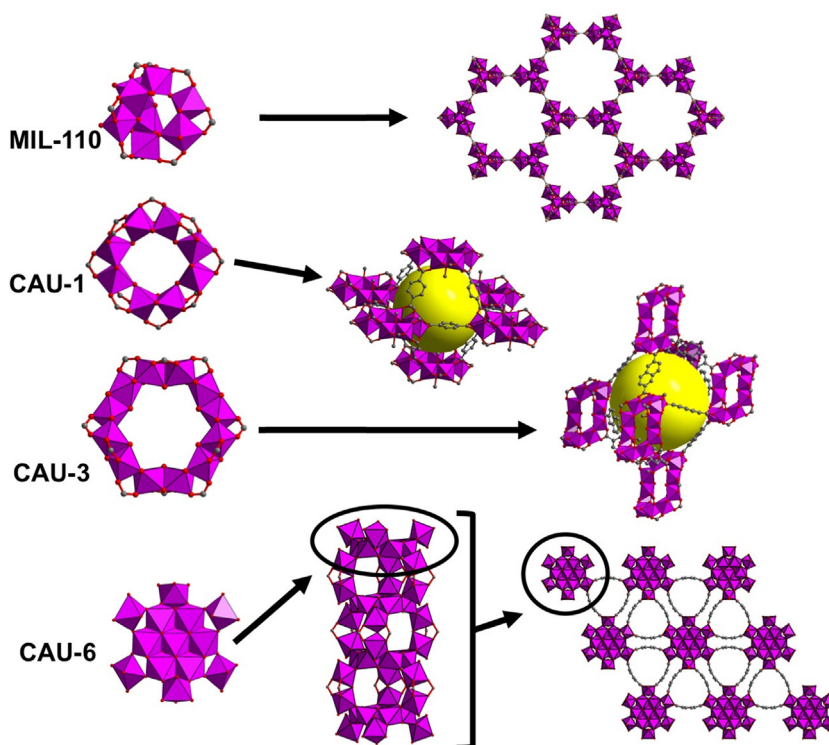
Fig. 4. (Color online.) Views of the different structures involving polynuclear aluminium-based subunits, in MIL-110 (octanuclear), CAU-1 (octanuclear), CAU-3 (dodecanuclear) and CAU-6 (related to the flat Al_{13} cationic entity). Yellow spheres indicate the pore space within the octahedral cavities.

aluminium centers. The CAU-1 material was also prepared by using the 2,5-dihydroxy terephthalate linker, which induces the presence of –OH group (instead of –NH$_2$) lining the porous cavities [126], but did not change the BET surface area (1350 m^2/g). Other modified forms of CAU-1 have been prepared by increasing reaction times using microwave assisted solvothermal synthesis route [127]. Thus, the methylated CAU-1 compound has been isolated (Al$_4$(OH)$_2$(OMe)$_4$(NHCH$_3$_1,4-*bdc*)$_3$) with this protocol. Post-synthetic modification (PSM) has been applied on the amino-functionalized form of CAU-1 in order to produce the amide derivative with "NHCOCH$_3$" group attached to the benzyl cycle of the ditopic ligand.

4.4. Metal-organic frameworks with other polynuclear building units

Even if the hydrolysis of aluminium provides large polycationic moieties, such Al$_{13}$, Al$_{30}$,... polyoxo/hydroxo clusters (see paragraph 1), only a very few MOF-like compounds contain inorganic building units with so high nuclearities. Indeed, just two phases have been identified with aluminium. The first example was discovered from reaction in methanol medium. Besides CAU-1 [122], a second type of solid is identified from high-throughput investigations, developed by Stock (Kiel University, Germany) [128]. This novel phase, CAU-3 (or Al$_2$(OCH$_3$)$_4$(L) [129]) was obtained with a series of ditopic linkers: H$_2$L = terepthalic acid, (1,4-H$_2$*bdc*), 2-amino terephthalic (NH$_2$_1,4-H$_2$*bdc*) or 2,6-naphthalene dicarboxylic acid

(2,6-H$_2$*ndc*). The structure of CAU-3 is built up from the connection of 12-membered ring bricks, through the ditopic ligands. The dodecameric [Al$_{12}$(OCH$_3$)$_{24}$]$^{24+}$ unit consists of the connection of AlO$_6$ octahedral polyhedra via edge-sharing (through μ_2-OCH$_3$ bridges) with a *cis-trans* sequence (Fig. 4). The flat wheel-like building block is then connected via bidentate carboxylate functions of the ditopic molecules to provide a distorted fcc packing arrangement, with octahedral ($\varnothing \approx 11$ Å) and tetrahedral ($\varnothing \approx 10$ Å) cavities. The BET surface areas of the terephthalate and naphthalendicarboxylate versions are about 1550 m^2/g and 2350 m^2/g, respectively. Even new for the crystal chemistry of aluminium, this type of motif was previously reported with transition metals, such as Mn^{3+} or Cr^{3+} [130,131].

The second compound CAU-6 [132] is related to the flat Al$_{13}$ brick (Fig. 1c) associated with the 2-amino terephthalate in 2-propanol medium (instead of using methanol). The structure of CAU-6 (Al$_{13}$(OH)$_{27}$ (H$_2$O)$_6$(NH$_2$_1,4-*bdc*)$_3$·Cl$_6$·(C$_3$H$_7$OH)$_6$) is based on the connection of Al$_{13}$ building units, previously described in [Al$_{13}$(OH)$_{24}$(H$_2$O)$_{24}$]Cl$_{15}$·13H$_2$O [39] (see paragraph 1), with the 2-amino-terephthalate linkers. It consists of 7 Al(OH)$_6$ octahedra linked through edges, surrounded by 6 peripheral Al(OH)$_5$(H$_2$O) octahedral units, acting as bidentate bridges via corner-sharing with planar central heptanuclear core (Fig. 4). These 6 peripheral Al(OH)$_5$(H$_2$O) octahedra are alternatively pointing upward and downward the central heptanuclear subunit and are further connected to each other via corner-sharing mode,

in order to generate infinite columns, developed along the *c* axis of the resulting hexagonal network. This type of connection with the ditopic molecule generates sinusoidal trigonal channels with diameters ranging from 5 Å to 10 Å, and small cavities of ~ 2.4 Å diameter. The thermally activated CAU-6 (for removal of the trapped 2-propanol species) revealed a BET surface area of 620 m^2/g.

4.5. Metal-organic frameworks with infinite chain as building units

4.5.1. Trans connection mode of AlO$_4$(OH)$_2$ units in infinite chains

Most of the (Al)MOFs of this type exhibit crystal structures based on linear chains consisting of AlO$_4$(OH)$_2$ octahedral units, connected to each other through corner-sharing μ_2-OH groups, located in *trans* position. This particular inorganic infinite building units is present with many organic linkers and was firstly reported in the MIL-53(Al) [96] material. This part describes the MIL-53 structural archetype and their different derived structures.

4.5.1.1. The case study of MIL-53(Al). MIL-53 type exists with many trivalent metals (Sc^{3+} [133], V^{3+} [97], Cr^{3+} [98], Fe^{3+} [134,135], Al^{3+} [96], Ga^{3+} [136–138], In^{3+} [139]) in association with the terephthalate ligand (1,4-benzenedicarboxylate, noted 1,4-*bdc*). The first member of the series was identified with the trivalent vanadium (MIL-47 [97]), but the compound is then oxidized into the V^{4+} state upon heating under O$_2$ flow. The general chemical formula of MIL-53 is M^{3+}(OH)(1,4-*bdc*)·*X*, where *X* represents encapsulated species within the structure pores. The framework structure of the aluminium member and its thermal behavior are closely related to the chromium parent [98]. It corresponds to the connection of the infinite linear ribbons of trans-connected AlO$_4$(OH)$_2$ units, via the terephthalate linkers acting as a bidentate bridging mode between two adjacent aluminium centers, through the carboxylate arms (Fig. 5). It results in the generation of a three-dimensional network with lozenge-shape channels, which are parallel to the chain axis. The original MIL-53(Al) phase was obtained in water in the presence of terephthalic acid, after a hydrothermal treatment at 220 °C from aluminium nitrate precursor. A recent work has shown the production of MIL-53(Al) can also be achieved from three insoluble aluminium sources: alumina (Al$_2$O$_3$), aluminum hydroxide (Al(OH)$_3$) or boehmite (AlOOH) [140].

In its as-synthesized form, unreacted terephthalic acid molecules reside within the rhombic tunnels (dimensions 7.3 × 7.7 Å^2 – cell volume: 1383 Å^3) in a disordered manner, but can be evacuated from the structure upon heating at 275 °C. This thermal treatment generates a high-temperature anhydrous form (LP for large pore), stable up to around 500 °C, with large empty pores and an enlarged channel aperture (dimensions 8.5 × 8.5 Å^2 – cell volume of 1412 Å^3) (Fig. 5). The BET surface area is then about 1140 m^2/g.

Either by decreasing temperature [134] or by reversible rehydration at 300 K in ambient air, this LP form shrinks without any amorphous intermediary state into a narrow pores form (NP), the topology remaining the same. During the transition, the *b* parameter of the cell, which corresponds to the axis of the infinite AlO$_4$(OH)$_2$ chains, remains quasi-constant whereas the *a* and *c* cell parameters show opposite variations.

In the first case, the hysteretic LP → NP transition occurs by cooling around 125 K, with a cell volume of 864 Å^3, whereas the reverse second-order transition happens on heating between 325 and 375 K [141]. The hysteretic phenomenon was confirmed later by ^{129}Xe NMR spectroscopy [142,143]. When rehydratation is concerned at 300 K, the water molecules are located at the center of the channels and generate hydrogen bond interactions with the carboxyl oxygen atoms and the bridging μ_2-OH groups, which are responsible of the shrinkage. The cell volume is reduced to 947 Å^3 with an aperture of 2.6 × 13.6 Å^2 for the channels.

Note that a fluorinated analog [144] has also been synthesized in a LP form from AlF$_3$ as precursor, without this time any terephthalic acid trapped within the channels. In this compound, the bridging μ_2-OH groups are replaced by μ_2-F groups. The cell volume of the empty
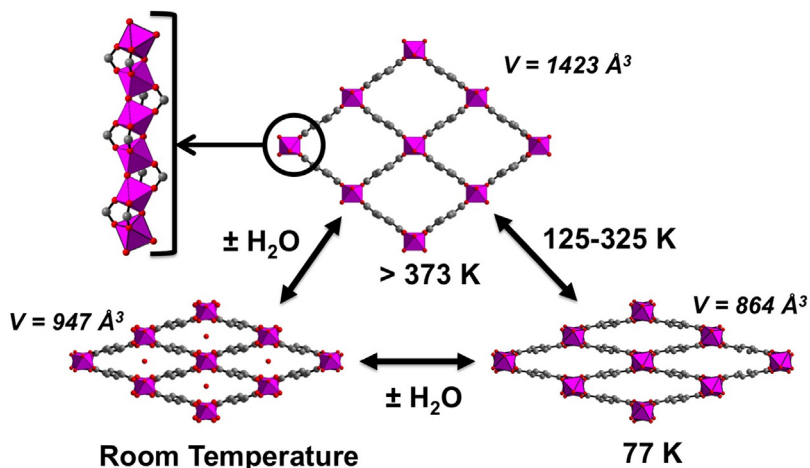

Fig. 5. (Color online.) Views of the structure-type MIL-53(Al) (also called Basolite™ A100) showing the pore size change as a function of temperature and/or hydration state.

pore is 1423 Å^3. The adsorption of various molecules (CCl$_4$, thiophene, cyclohexane,...) leads to a shrinkage dependent on the nature of the guest [145]. The most remarkable feature of MIL-53 type is indeed the unprecedented adaptability of its network to encapsulate a number of guest species with different sizes and characteristics. In the whole family adopting the MIL-53 structure type, the variation of the cell volume is always ca. 40%, the extreme values of the latter being 860 and 1500 Å^3. The extent of flexibility (also called the 'breathing effect') depends on several factors:

- the nature of the metallic cation in the chains;
- the chemical nature of the different guest molecules;
- the strength of the host-guest interactions within the tunnels [146].

Moreover, it was recently established by real-time environmental SEM analysis at the microscopic level [147] that the width and length of particles of the MIL-53(Al) crystallites vary during the transition.

The structural flexibility is not dedicated only to trivalent cations (see [135,136]) for example, but also exists with divalent transition metals, such as manganese, cobalt and nickel [148,149], when pyridine-N-oxide is used as a co-ligand.

Finally, MIL-53(Al) solids using either terephthalate or fumarate ligands are currently produced by BASF SE at the industrial scale and commercially available under the generic name Basolite^{TM} A100 and A-520 ([150] refs. therein). The BET surface area values are given for the range 1100–1500 m^2/g with a particle size distribution around 31.55 μm and are among the best materials for storage of natural gas at 300 K used as fuel in containers supplying cars (see below for more details).

4.5.1.2. Derivative structures of MIL-53(Al). Different strategies have been used for the elaboration of frameworks derived from the MIL-53(Al) structural archetype. They consist of the functionalization of the aromatic ring of the ditopic organic linker (here the terephthalate molecule). This can be done either by using pre-functionalized ligands or by modifying the ligand after the hydro/solvothermal synthesis (so-called post-synthetic modification protocol or PSM) of the MIL-53-like materials.

Using the first route, a series of solids with the various functionalities: –C$_4$H$_4$ (1,4-naphthalenedicarboxylate) [151], –NH$_2$ [116,117], –OH [152], –(COOH)$_2$ (also called MIL-121 [153]), –Cl, –Br, –CH$_3$, –NO$_2$, –(OH)$_2$ [154], –COOH [155], –F [156], have thus been prepared.

The other synthetic route is to perform successive organic reactions from a functionalized MIL-53 solid. The PSM method [157] has been applied successfully with the NH$_2$_MIL-53(Al) variant for the grafting of new chemical functions within the porous framework, thanks to the relatively good reactivity of pendant amino group. The addition of formic acid [116] leads to the formation of the corresponding amide MIL-53(Al) version. PSM highlighted also the better stability of NH$_2$_MIL-53(Al) compared to the amino version of MOF-5 (called IRMOF-3). Indeed, the

acidic by-product (HCl) generated by the reaction between amino groups from IRMOF-3 and phosgene derivatives leads to the decomposition and the solubilization of the zinc-based coordination polymer. The same conditions as those utilized with the NH$_2$_MIL-53(Al) allow the grafting of isocyanate (or isothiocyanate) functions and the conservation of the porous framework. Furthermore, the modified MIL-53 (noted MIL-53(Al)-NCO and MIL-53(Al)-NCS) are still able to support a second series of PSM after the addition of alcohols or amines, and the production of carbamates and urea functionalizations, respectively [158]. Attempts have been made with the HOOC_MIL-53(Al) compound, which can be partially decarboxylated into acid anhydride function (resulting from the condensation of two neighboring non-coordinating carboxylic acid groups) [155].

The MIL-53(Al) structure type can be obtained from diverse ditopic aromatic or aliphatic carboxylates with various lengths (Fig. 6). In this specific series, the two carboxylate functionalities are located at opposite positions either on the aromatic or alkyl chain of the spacer. The different solids with the "Al(OH)(L)" chemical formula are listed in the Table 1. It is observed that the non-porous NP form is obtained in MIL-69 [159], prepared in aqueous conditions, with 2,6-naphathalenedicarboxylic acid. Its dehydration process does not lead to the pore opening as it is observed for MIL-53, because of the presence of strong π–π interactions between the linkers. When DMF is used as solvent, the open form DUT-4 appears [160] (DUT stands for Dresden University of Technology), with a BET surface area of 1380 m^2/g, instead of non-porous phase for the hydrated MIL-69.

As expected, large pore windows have been observed with long ligands. For instance, with 4,4'-biphenyl dicarboxylate (DUT-5) [160], the aperture of the channels is 11.1 × 11.1 Å^2 (BET surface area of 1613 m^2/g). The naphthalene or biphenyl dicarboxylate can be used with different functionalities (–NO$_2$, –NH$_2$,...) or from pyridine fragment. In the latter, the reaction of 2,2'-bipyridine-5,5'-dicarboxylic acid with AlCl$_3$·6H$_2$O results in the formation of a DUT-5 analogous framework (also called MOF-253 [161]). The 2,2'-bipyridine function may act as a complexation site towards hetero-metallic elements, such as palladium dichloride (PdCl$_2$) or copper boron tetrafluoride (Cu(BF$_4$)), which increases the selectivity factor for binding CO$_2$ over N$_2$ from 2.8 (Pd) to 12 (Cu). In terms of length of dicarboxylate ligand, the smallest one is reported with fumaric acid, whose reaction in presence of aluminium salts was initiated by the BASF SE Company. Indeed, the resulting product, called Basolite^{TM} A520 [162] is fabricated at the industrial scale (up to 3600 kg/day) by using either the DMF [150] or water [163] as solvent. The authors expected the structure to be similar to that of MIL-53(Al) with the terephthalate groups replaced by fumarate linkers [164]. This was verified only very recently [165]. A520 exists in the NP form. The dimensions of the lozenge-shape channels are 5.7 × 6.0 Å^2 (BET surface area of 1080 m^2/g), but its aperture size does not change upon removing guest species, or heating. This is possibly due to the relatively rigid character of the fumarate ligand compared to that of terephthalate. The latter is known
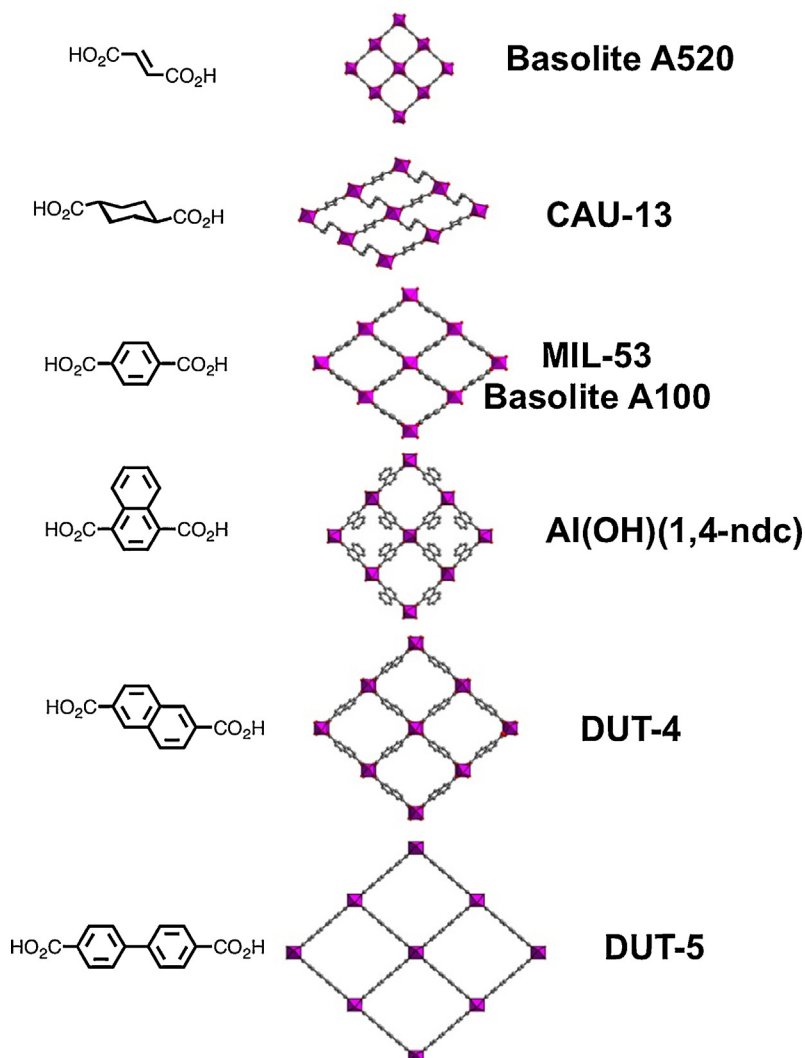
Fig. 6. (Color online.) View of the MIL53-like networks obtained with different ditopic carboxylate linkers (open pores are only represented, since for some of them, narrow pore systems may exist).

to have a possible rotation of benzene cycle regarding the carboxylate arms, which is not the case for the fumarate group. This type of MIL-53(Al)-based material, Basolite™ A520, has been selected by BASF SE for applications in the field of sorption. It has been used as sorbent for natural gas, in vehicles tanks. Compared with conventional container, the cruising distance is increased by 40% for a given pressure, with a container filled with Basolite™ A520 [162].

4.5.1.3. Other structural topologies with ditopic ligands. The infinite trans-connected $AlO_4(OH)_2$ chains building unit is also present in other types of topology (Table 1). In some cases, layered assemblies "Al(OH)(L)" have been isolated with infinite chains, interconnected via the ditopic molecules. The compounds MIL-129(Al) [170], Al(OH)(-cis-cdc) [171] and CAU-11 [172] have been obtained from the reactions of aluminium source with of 4,4′-azobenzenedicarboxylic acid, *cis*-1,4-cyclohexanedicarboxylic acid

(*cis*-H_2-*cdc*) and 4,4′-sulfonyl-dibenzoic acid, respectively. The latter shows a surface area of 350 m^2/g. In the CAU-11 version, also prepared by using the 3,3′,4,4′-diphenylsulfone-tetracarboxylic dianhydride, which hydrolyzes into tetracarboxylic acid, only two carboxylate arms are bonded to the $AlO_4(OH)_2$ chains, resulting in the functionalized *COOH*_CAU-11 phase [172].

However, other 3D networks have been identified with ditopic ligands (Fig. 7). For instance, with the terephthalate linker, a second structural variety exists, this time rigid (MIL-68), with the same formula Al(OH)(1,4-*bdc*)·X (X = solvent) as MIL-53. It represents a polymorph of the latter. Initially reported for trivalent vanadium [182], different analogs were produced latter with gallium [183], indium [183], iron [184] and scandium [185]. The MIL-68(Al) form, on its part, was established only recently [174], following a claim in a BASF patent [173]. MIL-68(Al) solid is obtained only from $AlCl_3 \cdot 6H_2O$ in *N,N*-dimethylformamide (DMF) after reflux thermal treatment at 130 °C for 18.5 h.

Table 1

List of the aluminium-based MOF compounds derived from the MIL-53 framework, using ditopic carboxylate ligands. Other topologies based on trans-connected $AlO_4(OH)_2$ octahedra infinite chains are also indicated.
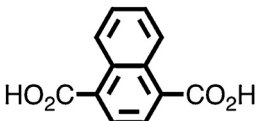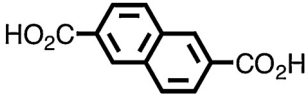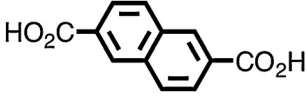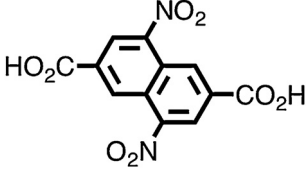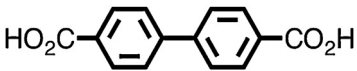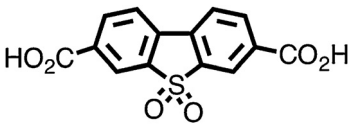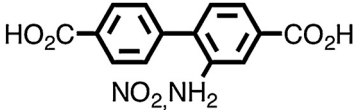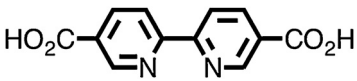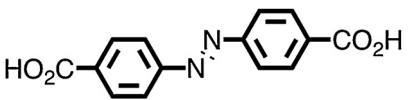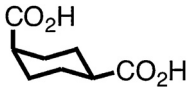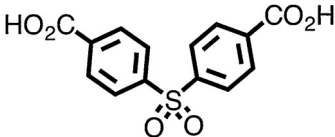
Code	Linker	Representation	Reference
MIL-53–like 3D networks			
MIL-53(Al) Basolite[TM] A100	1,4-Benzene dicarboxylic acid		[96]
/	1,4-Naphthalene dicarboxylic acid		[151]
MIL-69(Al)	2,6-Naphathalene dicarboxylic acid		[159]
DUT-4	2,6-Naphathalene dicarboxylic acid		[160]
MIL-69(Al)/DUT-4	1,5-Dinitro-3,7-naphathalene dicarboxylic acid		[166]
DUT-5	4,4′-Biphenyl dicarboxylic acid		[160]
SO₂_DUT-5	4,4′-Biphenyl-2,2′-sulfone-dicarboxylic acid		[166–168]
NH₂_DUT-5 NO₂_DUT-5	3-Amino or 3-nitro 4,4′-biphenyl dicarboxylic acid		[166]
MOF-253	2,2′-Bipyridine-5,5′-dicarboxylic acid		[161]
CAU-13	*trans*-1,4-Cyclohexane dicarboxylic acid		[169]
Basolite[TM] A520	Fumaric acid		[164,165]
Other topologies: 2D networks			
MIL-129	4,4′-Azobenene dicarboxylic acid		[170]
/	*cis*-1,4-Cyclohexane dicarboxylic acid		[171]
CAU-11	4,4′-Sulfonyl-dibenzoic acid		[172]

Table 1 (*Continued*)
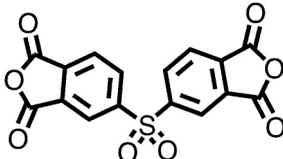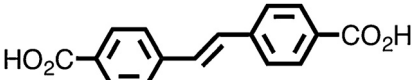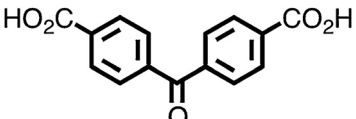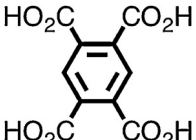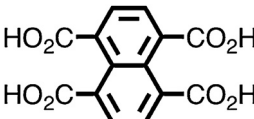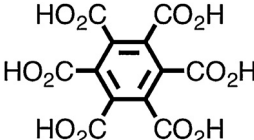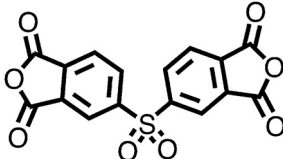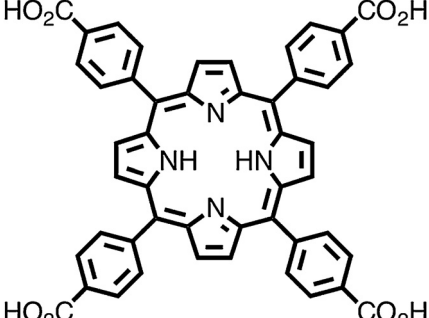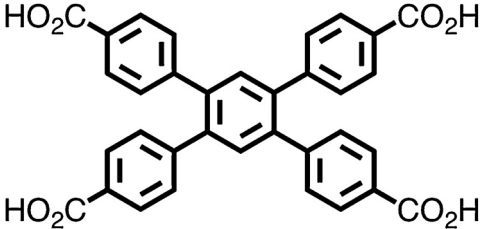
Code	Linker	Representation	Reference
*COOH*_CAU-11	3,3′,4,4′-Diphenylsulfone-tetracarboxylic dianhydride		[172]
Other topologies: 3D networks			
MIL-68(Al)	1,4-Benzene dicarboxylic acid		[173,174]
CYCU-3	4,4′-Stilbene-dicarboxylic acid		[175]
CAU-8	4,4′-Benzophenone-dicarboxylic acid		[176]
MIL-118	1,2,4,5-Benzene-tetracarboxylic acid		[177]
MIL-122	1,4,5,8-Naphthalene-tetracarboxylic acid		[178]
MIL-116	1,2,3,4,5,6-Benzene-hexacarboxylic acid		[179]
CAU-12	3,3′,4,4′-Diphenylsulfone-tetracarboxylic dianhydride		[172]
/	*meso*-Tetra(4-carboxyl-phenyl) porphyrin		[180]

Table 1 (*Continued*)

Code	Linker	Representation	Reference
CAU-9	1,2,4,5-Tetrakis-(-4-carboxylato-phenyl)-benzene		[181]

The structure type consists of the infinite chains of *trans*-connected $AlO_4(OH)_2$ octahedra linked to each other through the terephthalate ligand in such a way that hexagonal (16–17 Å apertures) and triangular channels (6.0–6.4 Å size), replace the distorted square channels of MIL(53). The BET surface area is 1430 m^2/g. It is typically a Kagomé topology composed of hexagonal rings surrounded by six triangular rings. The MIL-68(Al) member also crystallizes in tetrahydrofuran (THF) in contact of polysulfone for the preparation of mixed matrix membranes [186]. Also, an isoreticular network (called CYCU-3; Chung-Yuan Christian University, Taiwan) has been isolated [175] from the reaction of the 4,4′-stilbenedicarboxylic acid with aluminium chloride in DMF solvent. The use of this long diacid gives rise to an expansion of the MIL-68 framework, with large hexagonal mesoporous tunnels of 28×31 Å^2 aperture (BET surface area of 2757 m^2/g). These examples nicely illustrate the paramount influence of the nature of the solvent on the occurrence on dedicated phases, but the mechanisms at the molecular level involving such differences are yet unknown.

Finally, a second type of linker involves the use of two phenyl groups linked through a ketone function. It induces

Fig. 7. (Color online.) Views of the structure-type MIL-68, showing a Kagome-like lattice.

a V-shape conformation for this specific molecule (4,4′-benzophenonedicarboxylic acid), which gives rise to the generation of a complex three-dimensional framework with infinite chains of $AlO_4(OH)_2$ octahedra, running along two perpendicular directions. The resulting complex structure of compound (CAU-8 [176]) is built up from the alternation of two orthogonally oriented layered sub-networks of infinite chains, with non-intersecting channels (along [100] and [010]) of about 8 Å diameter. The BET surface area is 600 m^2/g.

4.5.1.4. Other structural topologies with tetratopic ligands. - The first member of Al-based MOF compounds involving tetradendate ligand has been obtained with the pyromellitate linker (1,2,4,5-benzenetetracarboxylate or *btec*) in the MIL-118 series [177] (Fig. 8). Surprisingly, the hydrothermal reaction of the pyromellitic acid with aluminium nitrate led to the formation of a three-dimensional framework composed of infinite chains of $AlO_3(OH)_2(H_2O)$ octahedral units linked to each other the tetratopic ligands. But, half of the carboxylate arms are bonded to aluminium centers by only one C-O-Al linkage, leaving free the second C-O bonding (acting as monodentate mode). This structural feature was not reported in the compounds based on ditopic ligands, for which each carboxylate arm adopts a bidentate bridging fashion with two adjacent aluminium centers. It could be correlated to the reaction pH and pK_a acidity constants of the tetratopic ligands. In fact, it was observed that in acidic solution (pH = 1.4), only half of the carboxylate is deprotonated allowing condensation reaction between aluminium and carboxylate groups (see MIL-121(Al) [153]). For MIL-118, the reaction pH is slightly higher (pH = 2) and it allows for the bidendate/monodentate connection mode of the carboxylate groups. At higher pH (12), all the carboxylate functions are deprotonated and fully connected with the aluminium centers. The resulting framework (MIL-120 [187]) will be discussed in Section 4.5.3. In MIL-118, the remaining non-bonded oxygen attached to aluminium is a terminal aquo species, which interacts via hydrogen bond with the free C–O bonding. Indeed, the gentle thermal treatment of MIL-118A (for as-synthesized product) at temperature between 150 and 170 °C, allows for the evacuation of water molecules together with the condensation of the aluminium center with the remaining non-bonding C–O. This topotactic transformation resulted in the fully connected pyromellitate ligands with chains of *trans*-connected $AlO_4(OH)_2$ octahedral units (MIL-118B)
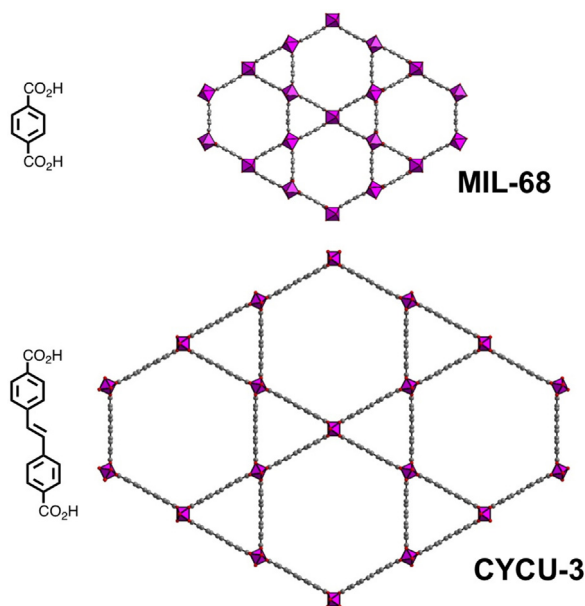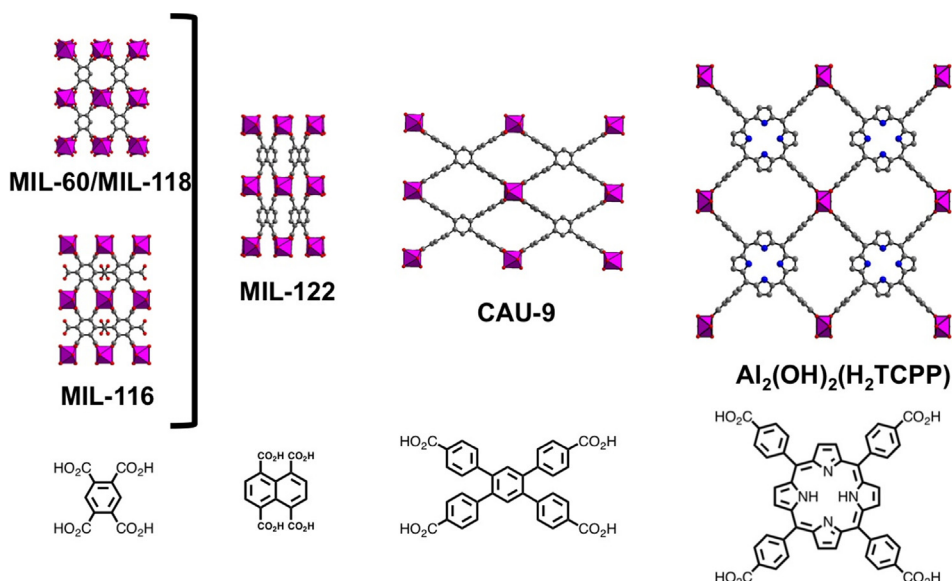
Fig. 8. (Color online.) Views of the aluminium-based MOF compounds obtained with various tetratopic carboxylate linkers.

with shrunk tunnels (3.5×1.5 Å^2). In this anhydrous form, the benzene planes of the organic ligand are tilted (angle $61°$), regarding the axis of the inorganic chains. But, at room temperature, the capture of water from ambient air atmosphere induces the shift of the inorganic chains to each other in order to get rectangular tunnels (angle $90°$), in which water molecules are encapsulated (MIL-118 C). The resulting structure exhibits one-dimensional channel systems, which is similar to the MIL-60 type, previously reported with vanadium [188] or indium [189].

From these MIL-118/MIL-60 archetypes, other MOF compounds with the generic formula "Al$_2$(OH)$_2$(L)" (Fig. 8) have then been produced by using various tetratopic ligands (Table 1). These different solids can be viewed as an isoreticular expansion of the MIL-60 net. Identical framework (MIL-116 [179]) is obtained with the 1,2,3,4,5,6-benzene hexacarboxylate linker (mellitate), for which two carboxylate functions remain under their protonated state (in 1,4-positions), and therefore it behaves as the pyromellitate ligand. With the use of 1,4,5,8-naphthalene-tetracarboxylate, the network MIL-122 [178] is produced as a shrunk form, without any porosity properties. A hydrated solid CAU-12 [172], is isolated with the 3,3′,4,4′-diphenyl-sulfone-tetracarboxylate ligand, for which two of the carboxylate arms are linked to aluminium centers in a monodentate fashion. Dehydration process of the coordinated water molecules led to the condensation of aluminium atoms with the non-bonded C–O, resulting in bidentate connection modes for all the carboxylate functionalities, following the reaction scheme observed in MIL-118. The porosity of these different compounds is quite low. However, attempts were successfully made with a tetradentate linker containing a porphyrin core [180]. In this case, the use of the *meso*-tetra(4-carboxyl-phenyl) porphyrin ligand led to the construction of a three-dimensional framework with infinite inorganic chains strictly perpendicular to the plane of the porphyrin core (Fig. 8). Due to the

large size of the ligand, elliptical channels are observed with 6×11 Å^2 aperture (along [010]), interconnected by other rectangular tunnels of 5×5 Å^2 along [001] and [110]. The BET surface area is about 1400 m^2/g. In this compound, the free-base porphyrin core is able to bind cationic metals, such as Zn^{2+} (occupancy up to 90%), which may possess enhanced photocatalytic properties. The last report described the use of 1,2,4,5-tetrakis-(4-carboxylato-phenyl)-benzene (*tcpb*) as tetratopic ligand and a similar three-dimensional network (CAU-9; Al$_2$(OH)$_2$(*tcbp*)·2DMF [181]) based on infinite *trans*-connected AlO$_4$(OH)$_2$ chains connected to each other via this linker, is generated (Fig. 8). The BET surface area is about 1120 m^2/g ($\varnothing = 4.5 \times 10.4$ Å).

4.5.2. Cis connection mode of AlO$_4$(OH)$_2$ units in infinite chains

The occurrence of a *cis* connection mode of AlO$_4$(OH)$_2$ octahedral units in chain-like systems is rather rare in the crystal chemistry of MOF-type solids. Indeed, the first illustration of such a chain was described in the indium pyromellitate MIL-117 [190]. More recently, this particular motif was uniquely found in the aluminium isophthalate CAU-10 (Al(OH)(*1,3-bdc*)·solvent −1,3-*bdc* = 1,3-benzene-dicarboxylate) [191], obtained in a mixed H$_2$O/DMF solvent. Its structure (Fig. 9) is built up from the association of infinite chains of AlO$_4$(OH)$_2$ octahedral units with the isophthalate linkers. The aluminium centers are connected to each other via two bridging μ_2-OH groups, located in *cis* positions within the octahedral geometry. These specific configurations of μ_2-OH groups generate infinite helices-like ribbons, which are arranged at the nodes of a square net. This 3D framework exhibits 6.8 Å channels (BET surface area = 635 m^2/g). Different versions of CAU-10 were later prepared with diverse functional groups (–CH$_3$, –OCH$_3$, –NO$_2$, –NH$_2$, –OH, –Br) located in the 5-position of the aromatic cycle of the isophthalate molecule. Starting mixtures of ligands, derived from the isophthalic acid,
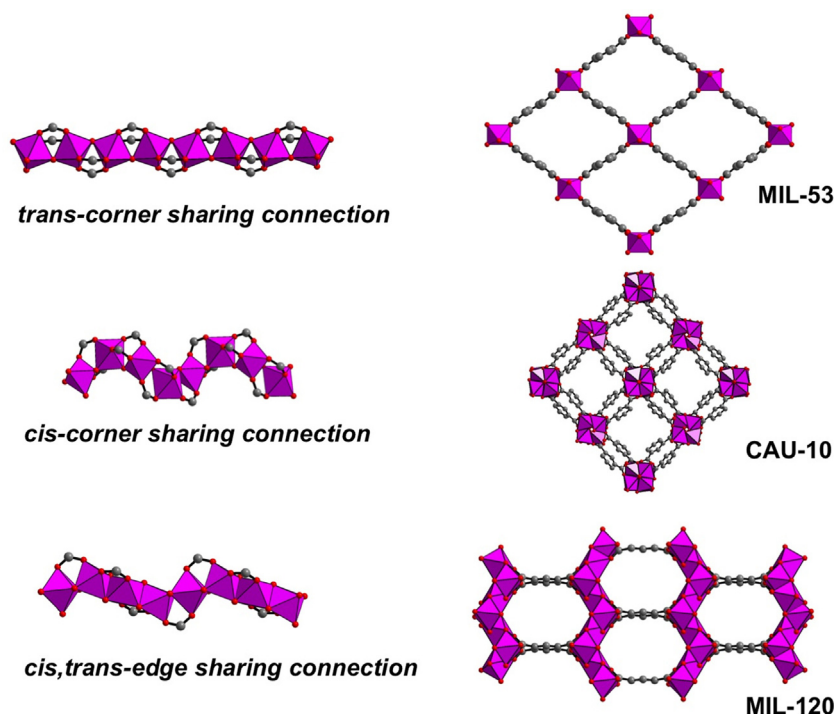
Fig. 9. (Color online.) Different connection mode of AlO_6 octahedral units involved in infinite chains and related networks (MIL53, CAU-10 and MIL-120).

were used with different functionalities and submitted to a solvothermal treatment. As a result, the CAU-10 topology incorporates couples of organic functions (ex: –H/–Br; –H/–CH$_3$; –NO$_2$/–NH$_2$/–NHCHO) [192].

4.5.3. Edge-sharing $AlO_2(OH)_4$ units in infinite chains

The *cis* connection fashion was also observed in another structural motif when octahedrally coordinated aluminium centers are linked together via edge-sharing. Again, this type of linkage is quite rare with light trivalent metals in MOF-type materials. It was firstly described in the aluminium pyromellitate MIL-120(Al), $Al_4(OH)_8(btec)\cdot 5H_2O$ $5H_2O$ (*btec* = 1,2,4,5-benzenetetracarboxylate) [187]. In this solid, $AlO_2(OH)_4$ octahedra are linked via double μ_2-OH bridges, generating either *cis* or *trans* positions in the chains (Fig. 9). The *cis/trans* sequence of the edge-sharing μ_2-OH bridge creates infinite zigzag ribbons, for which trans $AlO_2(OH)_4$ units strictly alternate with *cis* $AlO_2(OH)_4$ ones. All the carboxylate arms of the pyromellitate (acting as bidentate bridge between aluminium centers) ensure the connection of the inorganic chains to give a three-dimensional framework, with channels of ~ 5 Å diameter and a BET surface area of 308 m^2/g.

A related *cis-trans* edge-sharing arrangement was also observed in CAU-3 [129] but led to the formation of 12-membered wheel-like molecular building units instead of the infinite ribbons. For gallium, a layered compound (MIL-124(Ga)) is formed when trimellitic acid (1,2,4-benzene-tricarboxylic acid) is used. It contains the same infinite *cis-trans* edge-sharing $GaO_2(OH)_4$ octahedral units [193]. With aluminium, a similar bidimensional network has been

identified with phthalic acid (1,2-H$_2$*bdc*) in CAU-15 $(Al_4(OH)_8(1,2\text{-}bdc)_2\cdot H_2O)$ [194].

From these diverse examples, it is interesting to notice that the occurrence of 1,3 or 1,2-positions of the carboxylate functions of the linker seems to induce geometrical constraints, potentially favoring the formation of *cis* connection mode instead of *trans* one. It is the case for the fully deprotonated isophtalate, pyromellitate or phthalate ligands (or monoprotonated trimellitate acting as phthalate group in this case), but this cannot be taken as a general rule. Indeed, the 1,3,5-position for carboxylate functions (for instance with trimesate spacer) does not lead to any example of *cis* connection mode but to different types of motifs (see for instance the μ_3-oxo-centered trinuclear unit). On the contrary, the use of ditopic or large polytopic molecules seems to favor the formation of *trans*-connected $AlO_4(OH)_2$ straight chains in the corresponding structures.

5. Concluding remarks

This short review, beside its contribution to a better understanding of the crystal chemistry of aluminium, aimed at presenting a new strategy for the discovery of new topologies in the topical domain of often porous coordination polymers, starting from the knowledge of the known molecular species and their already described chemistry. It was shown that these latter could be used, alone or by condensation with others, as inorganic bricks for the design of new hybrid organic-inorganic phases [118,195–197]. However, one should notice that in the

case of aluminium compounds, the relation between molecular clusters and the building blocks of the nano-porous materials is scarcely direct, implying dynamical reorganization of the molecular species into the stabilized clusters in the crystals. This specificity is most probably related to water being a directly coordinated entity to aluminium leaving easily this coordination sphere. At desolvation stage during crystallization, for aluminium atoms, the water departure changes their coordination allowing a large reorganization of clusters. However, the strategy used here has led to numerous hitherto unknown solids in the ten last years, followed by their rational classification, once the numerous pertinent chemical parameters were evidenced. Both the originality of their structures, their low price and their significant thermal stability begin to inspire, for some of them, industrial applications helpful to the society.

References

[1] B.F. Hoskins, R. Robson, J. Am. Chem. Soc. 111 (1989) 5962.
[2] S.R. Batten, N.R. Champness, X.M. Chen, J. Garcia-Martinez, S. Kita-gawa, L. Ohrström, M. O'Keeffe, M. Paik Suh, J. Reedijk, Cryst. Eng. Commun. 14 (2012) 3001.
[3] J.R. Long, O.M. Yaghi, Chem. Soc. Rev. 38 (2009) 1213 (Themed issue on MOF).
[4] H.-C. Zhou, S. Kitagawa, Chem. Soc. Rev. 43 (2014) 5415 (Themed issue on MOF).
[5] H.-C. Zhou, J.R. Long, O.M. Yaghi, Chem. Rev. 112 (2012) 673 (Themed issue on MOF).
[6] G. Férey, Chem. Soc. Rev. 37 (2008) 191.
[7] G. Férey, C. Serre, C. Mellot-Draznieks, F. Millange, S. Surblé, J. Dutour, I. Margiolaki, Angew. Chem. Int. Ed. 43 (2004) 6296.
[8] G. Férey, C. Mellot-Draznieks, C. Serre, F. Millange, J. Dutour, S. Surblé, I. Margiolaki, Science 309 (2005) 2040.
[9] P. Horcajada, H. Chevreau, D. Heurtaux, F. Benyettou, F. Salles, T. Devic, A. Garcia-Marquez, C. Yu, H. Lavrard, C.L. Dutson, E. Magnier, G. Maurin, E. Elkaïm, C. Serre, Chem. Commun. 50 (2014) 6872.
[10] O.M. Yaghi, M. O'Keeffe, N.W. Ockwig, H.K. Chae, M. Eddaoudi, J. Kim, Nature 423 (2003) 705.
[11] H.W. Roesky, S.S. Kumar, Chem. Commun. (2005) 4027.
[12] C.W. Burnham, M.J. Buerger, Z. Kristallogr. 115 (1961) 269.
[13] L.B. Alemany, D. Massiot, B.L. Sherriff, M.E. Smith, F. Taulelle, Chem. Phys. Lett. 177 (1991) 301.
[14] A. Stephenson, P.B. Moore, Acta Cryst. B 24 (1968) 1518.
[15] S.G. Fleet, H.D. Megaw, Acta Cryst. 15 (1692) 721.
[16] Y. Kushi, Q. Fernando, J. Am. Chem. Soc. 92 (1970) 91.
[17] M.C. Cruickshank, L.S.D. Glasser, J. Chem. Soc., Chem. Commun. (1985) 84.
[18] G. Férey, T. Loiseau, P. Lacorre, F. Taulelle, J. Solid State Chem. 105 (1993) 179.
[19] N. Simon, J. Marrot, T. Loiseau, G. Férey, Solid State Sci. 8 (2006) 1361.
[20] T.W. Swaddle, J. Rosenqvist, P. Yu, E. Bylaska, B.L. Phillips, W.H. Casey, Science 308 (2005) 1450.
[21] N.N. Greenwood, A. Earnshaw, Chemistry of the Elements, 2nd ed., Butterworth-Heinemann, Elsevier, 2006.
[22] R.D. Shannon, Acta Cryst. A 32 (1976) 751.
[23] M.G. Goesten, G. Fonseca, C.F. Kapteijn, J. Gascon, BFM., Angew. Chem. Int. Ed. 54 (2015) 12034.
[24] W.H. Casey, Chem. Rev. 106 (2006) 1.
[25] R.B. Martin, Acc. Chem. Res. 27 (1994) 204.
[26] R.J.P. Williams, Coord. Chem. Rev. 149 (1996) 1.
[27] G. Berthon, Coord. Chem. Rev. 149 (1996) 241.
[28] V.B. Gupta, S. Anitha, M.L. Hegde, L. Zecca, R.M. Garruto, R. Ravid, S.K. Shankar, R. Stein, P. Shanmugavelu, K.S.J. Rao, Cell. Mol. Life Sci. 62 (2005) 143.
[29] W.H. Casey, B.L. Phillips, G. Furrer, Rev. Miner. Geochem. 44 (2001) 167.
[30] G. Johansson, Acta Chem. Scand. 16 (1962) 403.
[31] W.H. Casey, M.M. Olmstead, B.L. Phillips, Inorg. Chem. 44 (2005) 4888.
[32] G. Johansson, Acta Chem. Scand. 14 (1960) 771.
[33] G. Johansson, Acta Chem. Scand. 14 (1960) 769.
[34] G. Johansson, Arkiv. Kemi. 20 (1962) 305.
[35] G. Johansson, Arkiv. Kemi. 20 (1962) 321.

[36] J. Rowsell, L.F. Nazar, J. Am. Chem. Soc. 122 (2000) 3777.
[37] S. Abeysinghe, D.K. Unruh, T.Z. Forbes, Cryst. Growth Des. 12 (2012) 2044.
[38] S.E. Smart, J. Vaughn, I. Pappas, L. Pan, Chem. Commun. 49 (2013) 11352.
[39] W. Seichter, H.-J. Mögel, P. Brand, D. Salah, Eur. J. Inorg. Chem. (1998) 795.
[40] L. Pauling, Z. Kristallogr. 84 (1933) 442.
[41] L. Allouche, C. Gérardin, T. Loiseau, G. Férey, F. Taulelle, Angew Chem., Int. Ed. 39 (2000) 511.
[42] Z. Sun, H. Wang, H. Tong, S. Sun, Inorg. Chem. 50 (2011) 559.
[43] Z. Sun, H. Wang, Y. Zhang, J. Li, Y.-M. Zhao, W. Jiang, L. Wang, Dalton Trans. 42 (2013) 12956.
[44] W.H. Casey, J.R. Rustad, L. Spiccia, Chem. Eur. J. 15 (2009) 4496.
[45] J.-P. Jolivet, C. Chanéac, D. Chiche, S. Cassaignon, O. Durupthy, J. Hernandez, C.R. Geoscience 343 (2011) 113.
[46] A. Salifoglou, Coord. Chem. Rev. 228 (2002) 297.
[47] Z.L. Mensinger, W. Wang, D.A. Keszler, D.W. Johnson, Chem. Soc. Rev. 41 (2012) 1019.
[48] G.G. Bombi, B. Corain, A.A. Sheik-Osman, G.C. Valle, Inorg. Chim. Acta 171 (1990) 79.
[49] H. van Koningsveld, F.R. Venema, Acta Cryst. C 47 (1991) 289.
[50] F.R. Venema, H. van Koningsveld, J.A. Peters, H. van Bekkum, J. Chem. Soc., Chem. Commun. (1990) 699.
[51] C. Gabriel, M. Menelaou, M. Daskalakis, A. Lakatos, T. Kiss, C. Mateescu, R.G. Raptis, P. Zoumpoulakis, A. Salifoglou, Polehydron 27 (2008) 2911.
[52] D. Taylor, Aust. J. Chem. 31 (1978) 1455.
[53] R.G. Gillard, S.H. Laurie, P.R. Mitchell, J. Chem. Soc. (1969) 3006.
[54] J.C. Bailar Jr., E.M. Jones, Inorg. Synth. 1 (1939) 35.
[55] N. Bulc, L. Golic, J. Siftar, Acta Cryst. C 40 (1984) 1829.
[56] L. Golic, I. Leban, N. Bulc, Acta Cryst. C 45 (1989) 44.
[57] A. Tapparo, S.L. Heath, P.A. Jordan, G.R. Moore, A.K. Powell, J. Chem. Soc., Dalton Trans. (1996) 1601.
[58] M. Karlsson, D. Bostrom, L.-O. Öhman, Acta Chem. Scand. 52 (1998) 995.
[59] M. Karlsson, D. Bostrom, M. Clausen, L.-O. Öhman, Acta Chem. Scand. 52 (1998) 1116.
[60] W. Schmitt, P.A. Jordan, R.K. Henderson, G.R. Moore, C.E. Anson, A.K. Powell, Coord. Chem. Rev. 228 (2002) 115.
[61] S.P. Petrosyants, A.B. Ilyukhin, M.A. Malyarik, Zh. Neorg. Khim. 41 (1996) 1595.
[62] A.B. Ilyukhin, S.P. Petrosyants, S.V. Milovanov, M.A. Malyarik, Kristal-lografiya 42 (1997) 1034.
[63] G.C. Valle, G.G. Bombi, B. Corain, M. Favarato, P. Zatta, J. Chem. Soc., Dalton Trans. (1989) 1513.
[64] M. Matzapetakis, C.P. Raptopoulou, A. Terzis, A. Lakatos, T. Kiss, A. Salifoglou, Inorg. Chem. 38 (1999) 618.
[65] M. Matzapetakis, M. Kourgiantakis, M. Dakanali, C.P. Raptopoulou, A. Terzis, A. Lakatos, T. Kiss, I. Banyai, L. Iordanidis, T. Mavromoustakos, A. Saligoglou, Inorg. Chem. 40 (2001) 1734.
[66] T.N. Polynova, N.P. Bel'skaya, D. Turk de Garcia Banos, M.A. Prai-Koshits, L.I. Martynenko, Zh. Strukt. Khim. 11 (1970) 164.
[67] T.N. Polynova, L.A. Zasurskaya, A.B. Ilyukhin, Kristallografiya 42 (1997) 168.
[68] C. Robl, W.F. Kuhs, J. Solid State Chem. 92 (1991) 101.
[69] P. Sobota, M.O. Mustafa, J. Utko, T. Lis, J. Chem. Soc., Dalton Trans. (1990) 1809.
[70] S.P. Petrosyants, M.A. Malyarik, A.B. Ilyukhin, Zh. Neorg. Khim. 40 (1995) 769.
[71] M. Fairley, D.K. Unruh, A. Donovan, S. Abeysinghe, T.Z. Forbes, Dalton Trans. 42 (2013) 13706.
[72] S.L. Heath, P.A. Jordan, I.D. Johnson, G.R. Moore, A.K. Powell, M. Helliwell, J. Inorg. Biochem. 59 (1995) 785.
[73] A. Lakatos, R. Bertani, T. Kiss, A. Venzo, M. Casarin, F. Benetollo, P. Ganis, D. Facretto, Chem. Eur. J. 10 (2004) 1281.
[74] M. Dakanali, C.P. Raptopoulou, A. Terzis, A. Lakatos, I. Banyai, T. Kiss, A. Salifoglou, Inorg. Chem. 42 (2003) 252.
[75] A. Chrétien, E. Lous, Bull. Soc. Chim. Fr. 11 (1944) 446.
[76] F.A. Cotton, G. Wilkinson, Advanced Inorganic Chemistry, 5th ed., Wiley Interscience Publication, 1988.
[77] R.A. Reynolds III, W.O. Yu, W.R. Dunham, D. Coucouvanis, Inorg. Chem. 35 (1996) 2721.
[78] M.T. Andras, S.A. Duraj, A.F. Hepp, P.E. Fanwick, M.M. Bodnar, J. Am. Chem. Soc. 114 (1992) 786.
[79] C. Volkringer, T. Loiseau, Mater. Res. Bull. 41 (2006) 948.
[80] H. Hatop, M. Ferbinteanu, H.W. Roesky, F. Cimpoesu, M. Schiefer, H.-G. Schmidt, M. Noltemeyer, Inorg. Chem. 41 (2002) 1022.
[81] P. Lemoine, A. Bekaert, J.D. Brion, B. Viossat, Z. Kristallogr NCS 221 (2006) 309.

[82] W. Bury, E. Chwojnowska, I. Justyniak, J. Lewinski, A. Affek, E. Zygadio-Monikowska, J. Bak, Z. Florjanczyk, Inorg. Chem. 51 (2012) 737.
[83] T.L. Feng, P.L. Gurian, M.D. Healy, A.R. Barron, Inorg. Chem. 29 (1990) 408.
[84] S.A. Malone, P. Cooper, S.L. Heath, Dalton Trans. (2003) 4572.
[85] W. Schmitt, C.E. Anson, R. Sessoli, M. van Veen, A.K. Powell, J. Inorg. Biochem. 91 (2002) 173.
[86] O. Happel, K. Harms, A. Seubert, Z. Anorg. Allg. Chem. 633 (2007) 1952.
[87] U. Abram, D. Belli Dell'Amico, F. Calderazzo, S. Kaskel, L. Labella, F. Marchetti, R. Rovai, J. Strähle, Chem. Commun. (1997) 1941.
[88] J.B. Parise, Acta Cryst. C 40 (1984) 1641.
[89] J.J. Pluth, J.V. Smith, J.M. Bennett, J.P. Cohen, Acta Cryst. C 40 (1984) 2008.
[90] R. Nandini Devi, K. Vidyasagar, J. Chem. Soc., Dalton Trans. (1999) 3841.
[91] P.B. Moore, Am. Mineral. 57 (1972) 397.
[92] W. Schmitt, E. Baissa, A. Mandel, C.E. Anson, A.K. Powell, Angew Chem., Commun. 48 (2001) 3578.
[93] P. King, T.C. Stamatatos, K.A. Abboud, G. Christou, Angew Chem. Int. Ed. 45 (2006) 7379.
[94] P. O'Brien, H. Salacinski, M. Motevalli, J. Am. Chem. Soc. 119 (1997) 12695.
[95] J.C. Goodwin, S.J. Teat, S.L. Heath, Angew Chem. Int. Ed. 43 (2004) 4037.
[96] T. Loiseau, C. Serre, C. Huguenard, G. Fink, F. Taulelle, M. Henry, T. Bataille, G. Ferey, Chem. Eur. J. 10 (2004) 1373.
[97] K. Barthelet, J. Marrot, D. Riou, G. Férey, Angew Chem. Int. Ed. 41 (2002) 281.
[98] F. Millange, C. Serre, G. Férey, Chem. Commun. (2002) 822.
[99] S.T. Wilson, B.M. Lok, C.A. Messina, T.R. Cannan, E.M. Flanigen, J. Am. Chem. Soc. 104 (1982) 1146.
[100] H. Reinsch, M. Krüger, J. Wack, J. Senker, F. Salles, G. Maurin, N. Stock, Microporous Mesoporous Mater. 157 (2012) 50.
[101] S.R. Miller, P.A. Wright, C. Serre, T. Loiseau, J. Marrot, G. Férey, Chem. Commun. (2005) 3850.
[102] J. Perles, M. Iglesias, M. Martin-Luengo, M.A. Monge, C. Ruiz-Valero, N. Snejko, Chem. Mater. 23 (2005) 5837.
[103] M.T. Wharmby, M. Snoyek, T. Rhauderwiek, K. Ritter, N. Stock, Cryst. Growth Des. 14 (2014) 5310.
[104] T. Loiseau, L. Lecroq, C. Volkringer, J. Marrot, G. Ferey, M. Haouas, F. Taulelle, S. Bourrelly, P.L. Llewellyn, M. Latroche, J. Am. Chem. Soc. 128 (2006) 10223.
[105] C. Volkringer, D. Popov, T. Loiseau, G. Férey, M. Burghammer, C. Riekel, M. Haouas, F. Taulelle, Chem. Mater. 21 (2009) 5695.
[106] J.L. Schlenker, F.G. Dwyer, E.E. Jenkins, W.J. Rohrbaugh, G.T. Kokotailo, Nature 294 (1981) 340.
[107] C. Baerlocher, L.B. McCusker, D.H. Olson, Atlas of Zeolite Framework Types, 6th revised ed., Elsevier, Amsterdam, 2007, p. 228.
[108] M. Haouas, C. Volkringer, T. Loiseau, G. Férey, F. Taulelle, J. Phys. Chem. C 115 (2011) 17934.
[109] C. Volkringer, H. Leclerc, J.C. Lavalley, T. Loiseau, G. Ferey, M. Daturi, A. Vimont, J. Phys. Chem. C 116 (2012) 5710.
[110] E. Stavitski, M. Goesten, J. Juan-Alcaniz, A. Martinez-Joaristi, P. Serra-Crespo, A.V. Petukhov, J. Gascon, F. Kapteijn, Angew Chem. Int. Ed. 50 (2011) 9624.
[111] P. Serra-Crespo, E.V. Ramos-Fernandez, J. Gascon, F. Kapteijn, Chem. Mater. 23 (2011) 2565.
[112] C. Serre, F. Millange, S. Surblé, G. Férey, Angew Chem. Int. Ed. 43 (2004) 6286.
[113] C. Serre, C. Mellot-Draznieks, S. Surblé, N. Audebrand, Y. Filinchuk, G. Férey, Science 315 (2007) 1828.
[114] A.C. Sudik, A.P. Côté, O.M. Yaghi, Inorg. Chem. 44 (2005) 2998.
[115] M.G. Goesten, F. Kapteijn, J. Gascon, Cryst. Eng. Comm. 15 (2013) 9249.
[116] T. Ahnfeldt, D. Gunzelmann, T. Loiseau, D. Hirsemann, J. Senker, G. Ferey, N. Stock, Inorg. Chem. 48 (2009) 3057.
[117] J. Gascon, U. Aktay, M.D. Hernandez-Alonso, G.P.M. van Klink, F. Kapteijn, J. Catal. 261 (2009) 75.
[118] M.G. Goesten, P.C.M.M. Magusin, E.A. Pidko, B. Mezari, E.J.M. Hensen, F. Kapteijn, J. Gascon, Inorg. Chem. 53 (2014) 882.
[119] F. Millange, M.I. Medina, N. Guillou, G. Férey, K.M. Golden, R.I. Walton, Angew Chem. Int. Ed. 49 (2010) 763.
[120] C. Volkringer, D. Popov, T. Loiseau, N. Guillou, G. Ferey, M. Haouas, F. Taulelle, C. Mellot-Draznieks, M. Burghammer, C. Riekel, Nat. Mater. 6 (2007) 760.
[121] M. Haouas, C. Volkringer, T. Loiseau, G. Ferey, F. Taulelle, Chem. Eur. J. 15 (2009) 3139.
[122] T. Ahnfeldt, N. Guillou, D. Gunzelmann, I. Margiolaki, T. Loiseau, G. Férey, J. Senker, N. Stock, Angew Chem., Int. Ed. 48 (2009) 5163.
[123] H. Kumagai, S. Kitagawa, Chem. Lett. (1996) 471.

[124] R.H. Laye, M. Murrie, S. Ochsenbein, A.R. Bell, S.J. Teat, J. Raftery, H.-U. Güdel, E.J.L. McInnes, Chem. Eur. J. 9 (2003) 6215.
[125] M. Eshel, A. Bino, I. Felner, D.C. Johnston, M. Luban, L.L. Miller, Inorg. Chem. 39 (2000) 1376.
[126] T. Ahnfeldt, J. Moellmer, V. Guillerm, R. Staudt, C. Serre, N. Stock, Chem. Eur. J. 17 (2011) 6462.
[127] T. Ahnfeldt, D. Gunzelmann, J. Wack, J. Senker, N. Stock, Cryst. Eng. Comm. 14 (2012) 4126.
[128] H. Reinsch, N. Stock, Microporous Mesoporous Mater. 171 (2013) 156.
[129] H. Reinsch, M. Feyand, T. Ahnfeldt, N. Stock, Dalton Trans. 41 (2012) 4164.
[130] T.C. Stamatatos, A.G. Christou, C.M. Jones, B.J. O'Callaghan, K.A. Abboud, T.A. O'Brien, G. Christou, J. Am. Chem. Soc. 129 (2007) 9840.
[131] M. Helliwell, A.A. Smith, S.J. Teat, R.E.P. Winpenny, Inorg. Chem. Acta 354 (2003) 49.
[132] H. Reinsch, B. Marszalek, J. Wack, J. Senker, B. Gil, N. Stock, Chem. Commun. 48 (2012) 9486.
[133] J.P.S. Mowat, S.R. Miller, M.Z. Slawin, V.R. Seymour, S.E. Ashbrook, P.A. Wright, Microporous Mesoporous Mater. 142 (2011) 322.
[134] T.R. Whitfield, X. Wang, L. Liu, A.J. Jacobson, Solid State Sci. 7 (2005) 1096.
[135] F. Millange, N. Guillou, R.I. Walton, J.M. Grenèche, I. Margiolaki, G. Férey, Chem. Commun. (2008) 4732.
[136] C. Volkringer, T. Loiseau, N. Guillou, G. Férey, E. Elkaïm, A. Vimont, Dalton Trans. (2009) 2241.
[137] G. Chaplais, A. Simon-Masseron, F. Porcher, C. Lecomte, D. Bazer-Bachi, N. Bats, J. Patarin, Phys. Chem. Chem. Phys. 11 (2009) 5241.
[138] M. Vougo-Zanda, J. Huang, E. Anokhina, X. Wang, A.J. Jacobson, Inorg. Chem. 47 (2008) 11535.
[139] E.V. Anokhina, M. Vougo-Zanda, X.Q. Wang, A.J. Jacobson, J. Am. Chem. Soc. 127 (2005) 15000.
[140] Z. Li, Y.-N. Wu, J. Li, Y. Zhang, X. Zou, F. Li, Chem. Eur. J. 21 (2015) 6913.
[141] Y. Liu, J.-H. Her, A. Dailly, A.J. Ramirez-Cuesta, D.A. Neumann, C.M. Brown, J. Am. Chem. Soc. 130 (2008) 11813.
[142] A. Boutin, M.A. Springuel-Huet, A. Nossov, A. Gedeon, T. Loiseau, C. Volkringer, G. Ferey, F.X. Coudert, A.H. Fuchs, Angew Chem., Int. Ed. 48 (2009) 8314.
[143] M.A. Springuel-Huet, A. Nossov, Z. Adem, F. Guenneau, C. Volkringer, T. Loiseau, G. Ferey, A. Gedeon, J. Am. Chem. Soc. 132 (2010) 11599.
[144] L. Liu, X. Wang, A.J. Jacobson, Dalton Trans. 39 (2010) 1722.
[145] F. Millange, N. Guillou, M.E. Medina, G. Férey, A. Carlin-Sinclair, K.M. Golden, R.I. Walton, Chem. Mater. 22 (2010) 4237.
[146] C. Serre, G. Férey, Chem. Soc. Rev. 38 (2009) 1380.
[147] B. Seoane, S. Sorribas, A. Mayroral, C. Tellez, J. Coronas, Microporous Mesoporous Mater. 203 (2015) 17.
[148] G.H. Xu, X.G. Zhang, P. Guo, C.L. Pan, H.J. Zhang, C. Wang, J. Am. Chem. Soc. 132 (2010) 3656.
[149] A.S. Munn, G.J. Clarkson, F. Millange, Y. Dumont, R.I. Walton, Cryst. Eng. Comm. 15 (2013) 9679.
[150] C. Kiener, U. Müller, M. Schubert, patent 06112713.0/WO 2007/118841 (2006).
[151] A. Comotti, S. Bracco, P. Sozzani, S. Horike, R. Matsuda, J. Chen, M. Takata, Y. Kubota, S. Kitagawa, J. Am. Chem. Soc. 130 (2008) 13664.
[152] D. Himsl, D. Wallacher, M. Hartmann, Angew Chem., Int. Ed. 48 (2009) 4639.
[153] C. Volkringer, T. Loiseau, N. Guillou, G. Ferey, M. Haouas, F. Taulelle, E. Elkaim, N. Stock, Inorg. Chem. 49 (2010) 9852.
[154] S. Biswas, T. Ahnfeldt, N. Stock, Inorg. Chem. 50 (2011) 9518.
[155] N. Reimer, B. Gil, B. Marszalek, N. Stock, Cryst. Eng. Comm. 14 (2012) 4119.
[156] S. Biswas, T. Rémy, S. Couck, D. Denysenko, G. Rampelberg, J.F.M. Denayer, D. Volkmer, C. Detavernier, P. van der Voort, Phys. Chem. Chem. Phys. 15 (2013) 3552.
[157] S.M. Cohen, Chem. Rev. 112 (2012) 970.
[158] C. Volkringer, S.M. Cohen, Angew Chem., Int. Ed. 49 (2010) 4644.
[159] T. Loiseau, C. Mellot-Draznieks, H. Muguerra, G. Ferey, M. Haouas, F. Taulelle, C.R. Chimie. 8 (2005) 765.
[160] I. Senkovska, F. Hoffmann, M. Fröba, J. Getzschmann, W. Böhlmann, S. Kaskel, Microporous Mesoporous Mater. 122 (2009) 93.
[161] E.D. Bloch, D. Britt, C. Lee, C.J. Doonan, F.J. Uribe-Romo, H. Furukawa, J.R. Long, O.M. Yaghi, J. Am. Chem. Soc. 132 (2010) 14382.
[162] M. Gaab, N. Trukhan, S. Maurer, R. Gummaraju, U. Müller, Microporous Mesoporous Mater. 157 (2012) 131.
[163] E. Leung, U. Müller, N. Trukhan, H. Mattenheimer, G. Cox, S. Blei, patent WO 2012/042410 A1 (2012).
[164] F. Jeremias, D. Fröhlich, C. Janiak, S.K. Henninger, RSC Adv. 4 (2014) 24073.
[165] E. Alvarez, N. Guillou, C. Martineau, B. Bueken, B. Van de Voorde, C. Le Guillouzer, P. Fabry, F. Nouar, F. Taulelle, D. de Vos, J.-S. Chang, K.H.

Cho, N. Ramsahye, T. Devic, M. Daturi, G. Maurin, C. Serre, Angew Chem. Int. Ed 54 (2015) 3664.

[166] S. Halis, N. Reimer, U. Klinkebiel, N. Stock, Microporous Mesoporous Mater. 216 (2015) 13.

[167] S. Couck, Y.-Y. Liu, K. Leus, G.V. Baron, P. van der Voort, J.F.M. Denayer, Mic. Mes. Mater 206 (2015) 217.

[168] D.S. Raja, I.-H. Chang, Y.-C. Jiang, H.-T. Chen, C.-H. Lin, Microporous Mesoporous Mater. 216 (2015) 20.

[169] F. Niekel, J. Lannoeye, H. Reinsch, A.S. Munn, A. Heerwig, I. Zizak, S. Kaskel, R.I. Walton, D. de Vos, P. Llewellyn, A. Lieb, G. Maurin, N. Stock, Inorg. Chem. 53 (2014) 4610.

[170] C. Volkringer, T. Loiseau, T. Devic, G. Ferey, D. Popov, M. Burghammer, C. Riekel, Cryst. Eng. Comm. 12 (2010) 3225–3228.

[171] F. Niekiel, M. Ackermann, P. Guerrier, A. Rothkirch, N. Stock, Inorg. Chem. 52 (2013) 8699.

[172] N. Reimer, H. Reinsch, A.K. Inge, N. Stock, Inorg. Chem. 54 (2015) 492.

[173] M. Schubert, U. Müller, patent 07106802.7/WO 2008/129051 (2007).

[174] Q. Yang, S. Vaesen, M. Vishnuvarthan, F. Ragon, C. Serre, A. Vimont, M. Daturi, G. De Weireld, G. Maurin, J. Mater. Chem. 22 (2012) 10210.

[175] S.H. Lo, C.H. Chien, Y.L. Lai, C.C. Yang, J.J. Lee, D.S. Raja, C.H. Lin, J. Mater. Chem. A 1 (2013) 324.

[176] H. Reinsch, M. Krüger, J. Marrot, N. Stock, Inorg. Chem. 52 (2013) 1854.

[177] C. Volkringer, T. Loiseau, N. Guillou, G. Ferey, M. Haouas, F. Taulelle, N. Audebrand, I. Margiolaki, D. Popov, M. Burghammer, C. Riekel, Crystal. Growth Des. 9 (2009) 2927.

[178] C. Volkringer, T. Loiseau, N. Guillou, G. Ferey, E. Elkaim, Solid State Sci. 11 (2009) 1507.

[179] C. Volkringer, T. Loiseau, N. Guillou, G. Férey, D. Popov, M. Burghammer, C. Riekel, Solid State Sci. 26 (2013) 38.

[180] A. Fateeva, P.A. Chater, C.P. Ireland, A.A. Tahir, Y.Z. Khimyak, P.V. Wiper, J.R. Darwent, M.J. Rosseinsky, Angew Chem., Int. Ed. 51 (2012) 7440.

[181] M. Krüger, R. Siegel, A. Dreischarf, H. Reinsch, J. Senker, N. Stock, Microporous Mesoporous Mater. 216 (2015) 27.

[182] K. Barthelet, J. Marrot, G. Férey, D. Riou, Chem. Commun. (2004) 520.

[183] C. Volkringer, M. Meddouri, T. Loiseau, N. Guillou, J. Marrot, G. Férey, M. Haouas, F. Taulelle, N. Audebrand, M. Latroche, Inorg. Chem. 47 (2008) 11892.

[184] A. Fateeva, P. Horcajada, T. Devic, C. Serre, J. Marrot, J.M. Grenèche, M. Morcrette, J.-M. Tarascon, G. Maurin, G. Férey, Eur. J. Inorg. Chem. (2010) 3789.

[185] L. Mitchell, B. Gonzalez-Santiago, J.P.S. Mowat, M.E. Gunn, P. Williamson, N. Acerbi, M.L. Clarke, P.A. Wright, Catal. Sci. Technol. 3 (2013) 606.

[186] B. Seoane, V. Sebastian, C. Tellez, J. Coronas, Cryst. Eng. Comm. 15 (2013) 9483.

[187] C. Volkringer, T. Loiseau, M. Haouas, F. Taulelle, D. Popov, M. Burghammer, C. Riekel, C. Zlotea, F. Cuevas, M. Latroche, D. Phanon, C. Knofelv, P.L. Llewellyn, G. Ferey, Chem. Mater. 21 (2009) 5783.

[188] K. Barthelet, D. Riou, M. Nogues, G. Férey, Inorg. Chem. 42 (2003) 1739.

[189] C. Volkringer, T. Loiseau, G. Férey, Solid State Sci. 11 (2009) 29.

[190] M. Mazaj, C. Volkringer, T. Loiseau, V. Kaucic, G. Férey, Solid State Sci. 13 (2011) 1488.

[191] H. Reinsch, M.A. van der Veen, B. Gil, B. Marszalek, T. Verbiest, D. de Vos, N. Stock, Chem. Mater. 25 (2013) 17.

[192] H. Reinsch, S. Waitschat, N. Stock, Dalton Trans. 42 (2013) 4840.

[193] R. Hajjar, C. Volkringer, T. Loiseau, N. Guillou, J. Marrot, G. Férey, I. Margiolaki, G. Fink, C. Morais, F. Taulelle, Chem. Mater. 23 (2011) 39.

[194] H. Reinsch, D. de Vos, N. Stock, Z. Anorg. Allg. Chem. 639 (2013) 2785.

[195] M. Haouas, C. Volkringer, T. Loiseau, G. Férey, F. Taulelle, Chem. Mater. 24 (2012) 2462.

[196] G. Férey, M. Haouas, T. Loiseau, F. Taulelle, Chem. Mater. 26 (2014) 299.

[197] X. Yang, A.E. Clark, Inorg. Chem. 53 (2014) 8930.